

Stealth Engineering for *In Vivo* Drug Delivery Systems

Ankita Mohapatra,^{1,*} Bashir I. Morshed,² Warren O. Haggard,³ & Richard A. Smith⁴

¹Department of Electrical and Computer Engineering, University of Memphis, Memphis, TN 38152; ²Department of Electrical and Computer Engineering, University of Memphis, Memphis, TN 38152; ³Chair Excellence Associate Dean, Department of Biomedical Engineering, University of Memphis, Memphis, TN 38152; ⁴Department of Orthopedic Surgery & Biomedical Engineering, University of Tennessee Campbell Clinic, Memphis, TN 38163

*Address all correspondence to: Ankita Mohapatra, 3563 Poplar Avenue, #3, Memphis, TN 38111; Tel.: 901-343-1682; Fax: 901-678-5468; mhapatra@memphis.edu

ABSTRACT: In generic terms, a drug delivery substrate (DDS) can be described as a vehicle to transport drug to the point of interest. A DDS that would ideally have the capability to control drug dosage and achieve target specificity, localization, and higher therapeutic efficacy has been pursued as a holy grail in pharmaceutical research. Over the years, diverse classes, structures, and modifications of DDS have been proposed to achieve this aim. One of its major deterrents, however, is rapid elimination of drug by the immune system before intended functionality. Stealth engineering is broadly defined as a method of designing a drug carrier to minimize or delay opsonization until the encapsulated drug is delivered to the intended target. Stealth-engineered DDS has been successful in extending drug circulation lifetime from a few minutes to several days. Currently, this field of research has made much progress since its initiation in 1960s with liposomes to DNA boxes. Activity has also benefited several areas of medicine, where it has been applied in cancer, gene therapy, bone regrowth, and infection treatment. This review covers the progress of some types of DDS that have been published and indexed in major databases (including ScienceDirect, PubMed, and Google Scholar) in the scientific literature.

KEY WORDS: stealth engineering, drug delivery substrate, mononuclear phagocytic system, liposomes, polymeric micelles, dendrimers, viral capsid, deoxyribose nucleic acid, red blood cell

ABBREVIATIONS: **ADR**, Adriamycin; **CPT**, camptothecin; **DDS**, drug delivery substrate; **DNA**, deoxyribose nucleic acid; **GM1**, monosialoganglioside; **mPEG**, methoxy polyethylene glycol; **MPS**, mononuclear phagocytic system; **NP**, nanoparticle; **PX**, poloxamine; **PAMP**, pathogen-associated molecular patterns; **PC**, phosphatidylcholine; **PEG**, polyethylene glycol; **PEI**, polyethyleneimine; **PEO**, polyethylene oxide; **PLA**, polylactic acid; **PLGA**, poly(lactic-co-glycolic) acid; **RBC**, red blood cell; **RES**, reticulo-endothelial system; **ROS**, reactive oxygen species; **SM**, sphingomyelin; **SPIO**, super paramagnetic iron oxide; **TLR**, toll-like receptor; **TNF**, tumor necrosis factor; **VEGF**, vascular endothelial growth factor

I. INTRODUCTION

Since the latter half of the 20th century, there has been an escalating interest in developing an ideal drug carrier that could be injected intravenously, endure a long circulation period, and release drug in a controllable manner. This could facilitate external monitoring and regulation of drug dosage without causing the discomfort of repeated bolus injections to the patient. In addition, target-specific drugs could be administered easily without degradation *in vivo* before the intended delivery period. Numerous types of systems have been developed for this purpose; however, most suffer from surface opsonization by plasma proteins and elimination from circulation.

A. Mononuclear Phagocytic System

The mononuclear phagocytic system (MPS), traditionally referred to as reticulo-endothelial system (RES), is a part of the immune system consisting of cells that originate in bone marrow and ultimately settle in tissues as macrophages. The monocyte/macrophage cell family has a key role in the body's innate and adaptive immune responses and is on the front line for detection of foreign molecules and pathogens. Macrophages are a complex heterogeneous group of cells found throughout the body that provide a vast number of functions. The monocytes migrate from the blood into tissue to replenish long-lived tissue-specific macrophages of the bone (osteoclasts), alveoli, central nervous system (microglial cells), connective tissue (histiocytes), skin (Langerhans),

gastrointestinal tract, liver (Kupffer cells), spleen, and peritoneum.¹ These cells are phagocytic and search for older, worn out, or damaged cells such as erythrocytes (to conserve iron and hemoglobin) and virally infected cells to clear them from the circulatory system.² They also remove cellular debris from cells such as neutrophils, that have undergone apoptosis, as well as foreign debris including that from implanted biomaterials.³ Macrophage phagocytic actions replenish this debris ceaselessly from the tissue without producing inflammatory or immune mediators.⁴ However, debris from cells that have undergone necrosis yield molecular danger signals such as mRNA and heat shock proteins that activate the macrophages to secrete proinflammatory cytokines.⁵ The role of classically activated macrophages in host defense to intracellular pathogens has been well documented.^{1,6-8} Classically activated macrophages release growth factors, such as platelet-derived growth factor (PDGF) and vascular endothelial growth factor (VEGF) to initiate repair, and produce inflammatory cytokines such as tumor necrosis factor α (TNF α), MIF, interleukin-1 α (IL-1 α), IL-6, IL-8, and inducible nitric oxide synthase (iNOS or NOS2) to activate cellular programs, amplifying their own and other immune cells' antimicrobial activities. IL-1 and IL-6 mobilize other immune cells.²

Macrophages detect these danger signals specifically through toll-like receptors (TLRs), intracellular pattern-recognition receptors, and the IL-1 receptor.^{4,9,10} These have evolved over millions of years to detect pathogen-associated molecular patterns (PAMPs) related to pathogenic molecules such as lipopolysaccharide, lipoteichoic acid, and muramyl peptides derived from peptidylglycans. TLR activation then initiates signals (e.g., interleukin-receptor-associated kinases 1 and 4), activating the transcription factor NF- κ B and regulating inflammatory gene expression.^{11,12} These macrophages detect the bacteria in this process and become primed and activated, yielding microbicidal oxygen radicals such as superoxide anions, oxygen, and nitrogen-free radicals that kill pathogens as well as proinflammatory cytokines such as IL-6, IL-23, IL-1 β , and TNF α . Enhanced release of superoxide has also been shown to occur in response to interferon γ (IFN γ), irradiation, pH, osmolarity, and temperature changes.¹³⁻¹⁶

The body has a number of different molecules such as complement proteins, fibronectin, and vitronectin that may associate with biomaterials or in-

duced molecules.¹⁷ The interactions of these endogenous proteins with biomaterial may change the nature of the two components such that local macrophages may become activated. Therefore, avoiding or regulating macrophage priming and activation in a way that would inhibit the activity of other immune cells is a goal of stealth molecule technology. One possible group of regulatory molecules is the prostaglandins (PG). High concentrations of PG E₂ (PGE₂) are found at sites of infection, where it inhibits macrophage proinflammatory functions such as phagocytosis, reactive oxygen species (ROS) production, release of antimicrobial peptides, and production of TNF α , macrophage inflammatory protein 1 α , and leukotriene (LKT) B₄, but it enhances the production of anti-inflammatory IL-10.^{18,19} PGE₂ also inhibits ROS and LKT production by neutrophils and may enhance production of endogenous IL-10, which down-regulates dendritic cell functions.^{20,21} Finally, PGs inhibit fibroblast collagen and fibronectin synthesis and PDGF-stimulated migration.^{22,23}

Stealth engineering is the generic term assigned to drug delivery substrate (DDS) modification to delay its opsonization and ultimately renal elimination. This review provides a summary of recent research in stealth engineering for *in vivo* DDS, which is of particularly high interest for many therapeutic applications including chemotherapy for cancer, tumor treatment, bone regeneration, and blood sugar management.

B. Need for Stealth Engineering

The foundation for DDS was probably laid by Bangham et al., who reported selective restriction to diffusion of cations by swollen bilayer oolecithin structures,²⁴ also known as Bangasomes or liposomes. This was followed by abundant research on these structures.²⁵⁻³² Several other investigators proposed other DDS structures, such as dendrimers, polymer nanoparticles (NPs), micelles, and red blood cells.

From ingestion to final therapeutic activation, a drug carrier encounters several deterrent factors. Segal et al. injected radiolabeled compounds entrapped by liposomes in rat testicle and recorded testicular radioactivity, attributing the liberation to probable macrophageal endocytosis.²⁷ Carrier characteristics such as surface chemistry, charge, flexibility, size, and shape have an acute influence on *in vivo* lifetime. Designing an optimal carrier for

maximal efficacy is a vast research area in itself and has been explored extensively. It was suggested that adsorption of plasma protein on the surface of a drug particle caused clearance from circulation, after observing protein-binding behavior *in vivo* and *in vitro*; a higher capability to bind protein was associated with faster clearance kinetics.^{33,34} The protein was suggested to consist of high amounts of opsonin that triggered phagocytic uptake by the MPS. Particles of size >200 nm were observed to accumulate in spleen, whereas those <10 nm were prone to glomerular filtration.^{35–37} In addition, because the glomerular membrane contains anionic polysaccharides, cationic particles are sieved more quickly than anionic particles.³⁷ Hydrophobicity is another aspect that can prematurely terminate vasculature circulation and is usually solved by grafting hydrophilic polymers onto the carrier surface.^{36–40} Increased flexibility and branching of these steric shields further decrease macrophageal recognition by creating a high-density conformational barrier. NP shapes are also observed to affect pharmacokinetic behavior. Discher et al. showed that filamentous micelles had longer circulation than chemically similar spherical polyethylene-glycolated vesicles.⁴¹ Champion and Mitragotri fabricated worm-like polystyrene particles with high aspect ratios (>20) and reported negligible phagocytosis, compared to that of spherical particles of the same volume (1–3 μm diameter), when tested against a rat alveolar macrophage cell line.⁴² They attributed this to reduction in curvature and limiting to only the endpoints of the worm shapes, which theoretically in turn should decrease phagocytosis.

Early attempts to curb phagocytic reaction to drug carriers by temporarily causing MPS blockade occurred by administering a predose of similar particles. Researchers in 1980 studied the effect of an intravenous high dose of empty multilamellar liposomes on opsonization rate of a second dose encapsulating ¹⁴C-inulin injected at 1, 5, and 24 h.⁴³ They observed that in comparison to a control group for which only the second dose was given, ¹⁴C-inulin level in blood increased by a factor of 29 and decreased by a factor of 6 in liver when a preemptive dose was administered 1 h before actual dose. A similar method describes injecting a predose of large unilamellar liposomes to limit the clearance of the second drug dose.⁴⁴ Furthermore, different sizes of liposomes were comparatively studied to

understand the dependency, if any, of MPS flushing on particulate size of such consecutive doses.^{45,46} Small liposomes (40–200 nm) were shown to have a relatively higher circulation when compared to their larger counterparts.

Dextran sulphate (DS) was also used to lower the rate of clearing foreign particles from the bloodstream by impeding MPS functioning, in some cases even resulting in absolute cessation of immunological response.^{47,48} Patel et al. demonstrated a suppression of liver uptake of multilamellar liposomes by injecting a maximal dose of 50 mg DS/kg body weight that caused a temporary liver blockage lasting 48 h.⁴⁹ Liver uptake was observed to have dropped as early as 2 h after infusion of DS. Prior dosage of a monoclonal antibody such as 2.4G2 demonstrated an inhibition in clearance of liposomes loaded with dinitrophenyl.⁵⁰

The half-life and area under the plasma-concentration time curve provide an accurate assessment of how long the DDS survives *in vivo*. Toutain and Bousquet-Melou defined plasma terminal half-life as, "...following intravenous (IV) administration, the terminal half-life is the time required for plasma/blood concentration to decrease by 50% after pseudo-equilibrium has been reached; then, terminal half-life is computed when the decrease in drug plasma concentration is due only to drug elimination, and the term elimination half-life is applicable."⁵¹ Zhang et al. published a detailed 2013 review of materials that have been tested for drug delivery along with FDA approval dates for those that were successful.⁵²

In this article, we review some DDSs that have been widely studied. Table 1 summarizes important data of various formulations reported. The data provided are not intended to highlight a negative comparison among adequacies; they simply serve to provide knowledge about various developmental approaches to DDS. Data were primarily collected and summarized from the databases maintained through FDA archives and the Drugbank of Canada. Figure 1 shows a layout of this review.

II. ARTIFICIAL STEALTH ENGINEERING TECHNIQUES FOR *IN VIVO* DRUG DELIVERY

Various types of polymers and other biological entities have been artificially developed for the required

TABLE 1: Summary of DDS stealth-engineered products developed in recent years for in-vivo applications

Type	Name of Product	Drug Load	Constituents of modification	Size	Elimination		Plasma AUC (before)	Plasma AUC (after)	Injected Dose	Test Subjects	References
					half-life of drug before modification	half-life of drug after modification					
Polymeric micelle	Genexol	Paclitaxel	mPEG-PDLLA	<50 nm	0.98-1.84 h (dose dependent)	11.0-17.9 h (dose dependent)	n.a.	27490 ± 8.297 ng/h/mL	390 mg/mm ²	Humans	39,53,54
	NK105	Paclitaxel	PEG-P(Asp)	85 nm	0.98-1.84 h (dose dependent)	5.99-6.82 h (dose dependent)	309.0 µg/h/mL	15573.6 µg/h/mL	100 mg/kg	26-Bearing CDF1 mice	39,53,54
	NC-6004	Cisplatin	PEG-P(Glu)	30 nm	20-30 min	6.43 h	75.73 ± 26.13 µg/h/mL	1335.47 ± 75.99 µg/h/mL	5 mg/kg	BALB/c Nude rats implanted with MKN-45 cancer cell line	39,55, Drugbank
	NK911	Doxorubicin	PEG-P(Asp)	40 nm	5-10 min	1.6-4.7 h	1620.3 ± 1062.9 ng/h/mL	4174.1 ± 471.2 ng/h/mL	50 mg/mm ²	Humans	39,56
Liposome	SP1049C	Doxorubicin	Pluronic F127, L61	30 nm	5-10 min	48.8 h	1620.3 ± 1062.9 ng/h/mL	~2190 ng/h/mL	50 mg/mm ²	Humans	39,56,57
	Pluronic 85	Doxorubicin	ABA type of PPO and PEO	n.a.	5-10 min	90 h (for 1% weight dose)	n.a.	1045 µg/h/mL	1% weight	C57/BL/6 Mice	39,58
	Ps10	FTIC-dextran	PEG-PDLLA::10:90	96.3 ± 6.6 nm	<2 h	47 ± 12.7 h	n.a.	2634 ± 258 %ID/h/mL	100 mg/kg	C57BL/6J Female mice	59
	-	ADR	PEG-P(Asp)	50 nm	18 min (at 10 mg/kg)	70 min	n.a.	n.a.	0.1 mL/10 g	C57BL/6 Male mice	60
Liposome	tHA-LIP	Doxorubicin	Hyaluronan	81 nm	5-10 min	139 h	-	tHA-LIP/free DXR = 47	10 mg/kg	Mice	61
	Stealth liposome®	1-β-D-Arabinofuranosylcytosine	HSPEC:CH:PEG-DSPE::2:1:0.1	400 nm	16-20 min	12 h	n.a.	n.a.	0.5 µmol	Leukemia-bearing mice	62

TABLE 1: (continued)

Type	Name of Product	Drug Load	Constituents of modification	Size	Elimination half-life of drug before modification	Elimination half-life of drug after modification	Plasma AUC (before)	Plasma AUC (after)	Injected Dose	Test Subjects	References
	Conventional liposomes	-	PC:CH::2:1	92-123 nm	-	13 h	-	89295 nmol/h/mL	10 μ mol	Female mice	63-65
	Stealth liposome®		SM:PC:CH:GM1::1:1:1:10%			21.6 h		138754 nmol/h/mL			
	Stealth liposome®		SM:PC:CH:PEG-DSPE::1:1:1:10%			24.8 h		170150 nmol/h/mL			
	Conventional liposomes	Flurbiprofen	SPC:cholesterol::4:1	168 nm	2.31 h	7.36 h	151650.7 \pm 16.760 ng/mL/h	43924.1 \pm 24.440 ng/mL/h	2.5 mg/kg	Male albino Wistar arthritic rats	66
	DSPC liposomes		DSPC:cholesterol::4:1	182 nm		7.84		512,669 \pm 21,640 ng/mL/h			
	Stealth liposome®		DSPC:cholesterol:DSPE-PEG::4:1:0.2	192 nm		19.87 h		704408.3 \pm 77.430 ng/mL/h			
	Stealth liposome®	Mitoxantrone	DSPC:cholesterol:DPPE-PEG ₂₀₀₀ ::50:45:5	n.a	<30 min	n.a	11.51 μ mol h mL ⁻¹	28.27 μ mol h mL ⁻¹	10 mg/kg ⁻¹	Female BDF1 mice	67
	Conventional liposomes	-	PC:cholesterol::1:1	0.2 μ m	-	<30 min	n.a.	n.a	0.12-0.14 mg	Male Balb/c mice	63-65
	Stealth liposome®		PC:cholesterol:PEG-PE::1:1:0.16			5 h					
	Targeted stealth liposome® (transferrin)	Doxorubicin	DSPC:cholesterol:DSPE-PEG-COOH::6:3:0.6	70 \pm 19 nm	5.476 \pm 1.690 h	22.238 \pm 2.059	0.538 \pm 0.145 μ g/h/mL	1221.262 \pm 80.795 μ g/h/mL	5 mg/kg	Male ICR mice	68
	Stealth liposome®	FITC-dextran	DPPC:chol:PEG-DSPE::1.85:1:0.15)	103 nm	<2 h	10.6 \pm 1.8 h	n.a.	797 \pm 46 %ID/h/mL	70 mg/kg	C57Bl/6J Female mice	59
	Conventional liposomes	IBP 5823	PLA:albumin	160 nm	n.a.	2-3 min	n.a.	10 h/ μ g/mL	8 mg/kg	Sprague-Dawley rats	69
	Stealth liposome®		PLA:PEG	120 nm		6 h		120 h/ μ g/mL	7 mg/kg		
	Stealth liposome®	Monensin	DPPC:cholesterol:DSPE-PEG	114 \pm 32 nm	n.a.	7-8 h	n.a.	n.a.	0.7 μ mol lipid (total)	BALB/c Mice	70
	Stealth liposome®		DPPC:cholesterol:DSPE-PEG + anti-MY9 antibody	127 \pm 41 nm							

TABLE 1: (continued)

Type	Liposome	Name of Product	Drug Load	Constituents of modification	Size	Elimination half-life of drug before modification	Elimination half-life of drug after modification	Plasma AUC (before)	Plasma AUC (after)	Injected Dose	Test Subjects	References
SLN		Stealth liposome®	Radiolabeled	PHEPC:PEG-DSPE:HYNIC-DSPE: cholesterol:	900 nm	n.a.	43 h	n.a.	n.a.	0.5 µmol/kg	Humans	71
		OB2	-	1200 Da PEG	100 nm	-	15.8 ± 2.2 h	n.a.	n.a.	0.1 µmol/kg	Sprague-Dawley and Wistar rats	72
		OE7		1840 Da PEG			18.5 ± 4.7 h					
		OB16		2300 Da PEG			28.0 ± 10 h					
	Stealth SLN (SSLN)	OB18		3680 Da PEG			25.5 ± 2.7 h					
		Icariin		Cholesterol, PEG, lecithin	50.03 ± 0.90 nm	0.21 h	1.40 h	0.82 mg/h/L	3.34 mg/h/L	7.46 mg/kg	Kunming mice	73
		Doxorubicin		Stearic acid, epikuron 200	80 ± 5 nm	5-10 min	241.7 ± 95.3 min	83:70 ± 19:82 µg/min/mL	814.45 ± 46.11 µg/min/mL	6 mg/kg	Rats	74
	SSLN			Stearic acid, epikuron 200, PEG	90 ± 5 nm		211.2 ± 44.3 min	1121.10 ± 75.85 µg/min/mL				
		Liposomal doxorubicin (L-dox)/caelyx	Doxorubicin	PC, PEG-40-carbonyl-l-distearoyl phosphatidylethanolamine	12 nm	0.5 ± 0.1 h	23.6 ± 3.0 h	0.42 ± 0.07 µg/h/mL	1786 ± 367 µg/h/mL	2 mg/kg doxorubicin equivalent	Walker 256 tumor-bearing rats	75
Dendrimers	Dendrimer doxorubicin (D-dox)			Polylysine, PEG1100	89 nm		19.3 ± 3.1 h		341 ± 39 µg/h/mL			
	PEG ₄₅ -DiCPT	CPT		Polylysine, PEG	100 nm nano-sphere	-	1.61 h	-	47.13%ID/h/g	10 mg CPT equivalent/kg	BALB/c Mice	76
	PEG ₄₅ -tetraCPT				60 nm diameter, 500 nm long		5.82 h		239.71%ID/h/g			
	PEG ₄₅ -octaCPT				100 nm diameter, 1 µm long		1.70 h		58.2 %ID/h/g			

TABLE 1: (continued)

Type	Name of Product	Drug Load	Constituents of modification	Size	Elimination half-life of drug before modification	Elimination half-life of drug after modification	Plasma AUC (before)	Plasma AUC (after)	Injected Dose	Test Subjects	References
Dendrimers	DN1	Indomethacin (intra-peritoneal administration)	Folate-PAMAM conjugate, indomethacin = 932.0 ± 12.52 µg/mL	n.a.	3.09 ± 0.13 h	6.12 ± 0.78 h	91.93 ± 10.35 µg/h/mL	125.94 ± 22.34 µg/h/mL	3.3 mg/kg indomethacin equivalent	Arthritic Wistar rats	77
	FN1		Folate-PAMAM conjugate, indomethacin = 964.8 ± 14.96 µg/mL			7.80 ± 0.15 h		127.56 ± 25.19 µg/h/mL			
	FN2		Folate-PAMAM conjugate, indomethacin = 1393.8 ± 21.75 µg/mL			8.89 ± 1.94 h		121.22 ± 1.86 µg/h/mL			
	FN3		Folate-PAMAM conjugate, indomethacin = 1457.5 ± 20.28 µg/mL			8.17 ± 1.63 h		166.59 ± 0.20 µg/h/mL			
	DN1	Indomethacin (in inflamed paw)	Folate-PAMAM conjugate, indomethacin = 932.0 ± 12.52 µg/mL	n.a.	5.06 ± 0.42 h	11.79 ± 2.68 h	207.51 ± 15.42 µg/h/mL	396.44 ± 18.65 µg/h/mL	3.3 mg/kg indomethacin equivalent	Arthritic Wistar rats	77
	FN1		Folate-PAMAM conjugate, indomethacin = 964.8 ± 14.96 µg/mL			22.79 ± 3.15 h		579.01 ± 19.25 µg/h/mL			
	FN2		Folate-PAMAM conjugate, indomethacin = 1393.8 ± 21.75 µg/mL			29.92 ± 2.36 h		602.89 ± 22.18 µg/h/mL			
	FN3		Folate-PAMAM conjugate, indomethacin = 1457.5 ± 20.28 µg/mL			37.08 ± 2.94 h		850.73 ± 20.59 µg/h/mL			
	FN3		Folate-PAMAM conjugate, indomethacin = 1457.5 ± 20.28 µg/mL			8.17 ± 1.63 h		166.59 ± 0.20 µg/h/mL			

ADR, Adriamycin; AUC, area under curve; COOH, carboxyl functional group; CPT, camptothecin; DSPC, distearoylphosphatidylcholine; DPPC, dipeptide transport system permease protein; DSPE, 2-distearoyl-*sn*-glycero-3-phosphoethanolamine; DPPE, bis(diphenylphosphino)ethane; DXR, doxorubicin; FITC, fluorescein isothiocyanate; HSPC, hydrogenated soy phosphatidylcholine; IBP, injectable blood persistent (particulate); ID, injected dose; n.a., not available; mPEG, methoxy polyethylene glycol; NSLN, non-stealth SLN; PAMAM, polyamidoamine; PC, phosphatidylcholine; PDLA, poly(D,L)lactide; PEG, polyethylene glycol; PEO, polyethylene oxide; PHEPC, partially hydrogenated egg phosphatidylcholine; PLA, poly(lactic) acid; PPO, polypropylene oxide; SLN, solid-lipid nanoparticle; SPC, stearylphosphatidylcholine; SSLN, stealth SLN.

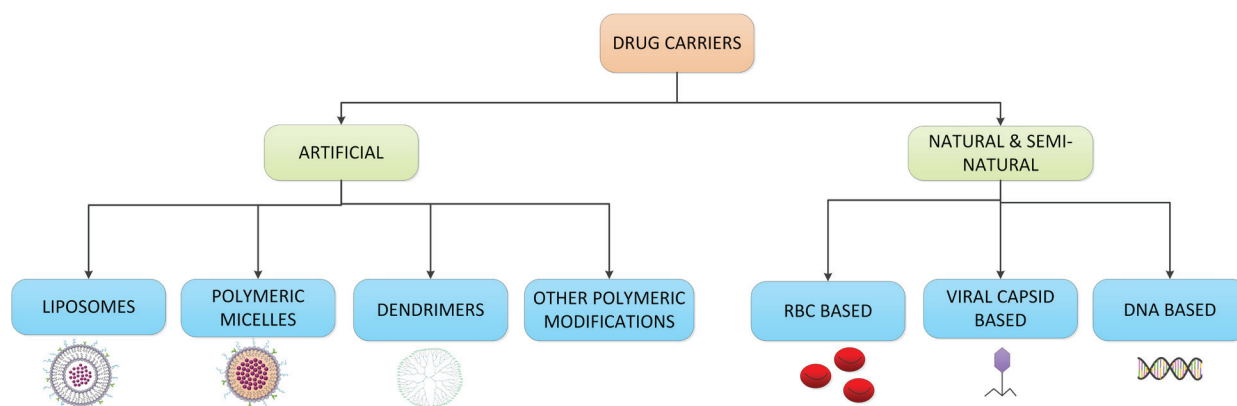


FIG. 1: Broad classification of the types of DDSs. Only major groups are shown here and discussed in this review.

camouflage ability of stealth-engineered DDS for *in vivo* applications. Some of these techniques have shown promise and have been tested in animal studies. Major stealth engineering techniques for *in vivo* DDS are discussed in this section.

A. Liposomes

Liposomes are phospholipid bilayers that encapsulate drug in the inner compartment, whereas the outer bilayer acts as its shield (Fig. 2). Some drugs can also be entrapped in the vesicular space. Liposomes were discovered by Bangham in 1961 and were extensively adopted as DDS, followed by various approaches to extend their short half-life *in vivo*. A comparative study of *in vivo* circulation time between nonentrapped neuraminidase and neuraminidase enclosed in liposomes with varying lipid concentration was done by Gregoriadis et al.³¹ These researchers reported a higher circulation time for liposomes with a higher constituent of lipids, thus concluding that the rate of renal elimination is dictated by the drug carrier, rather than by the drug itself. Furthermore, it was observed that cholesterol-rich liposomes displayed enhanced *in vivo* lifetimes over cholesterol-poor or cholesterol-nil liposomes by impeding serum opsonin binding.^{63–65} Semple et al. also noted that cholesterol inclusion improves packing density of liposomal phospholipid molecules, thereby decreasing ion permeability.⁶⁵

Negatively charged liposomes cleared faster when compared to neutral or positively charged liposomes; hence, the negative charge on liposomes was labeled as a probable factor of recognition by the MPS.³⁴ As a remedy for this, liposomes were

structured with a low molar fraction of a negatively charged glycolipid, such as monosialoganglioside (GM1)³⁴ or phosphatidylinositol, and a neutral phospholipid was used as the major constituent.⁷⁸ These modified liposomes that were termed sterically stabilized had a longer circulation time without MPS blockage. The effect of different concentrations of ganglioside and sphingomyelin (SM) modifications in liposomes on liver uptake was studied,^{34,79,80} and it was conclusively demonstrated that these modifications provided a longer lifetime *in vivo* than that of classical liposomes; they were called stealth liposomes. The liposomes of SM:phosphatidylcholine (PC):cholesterol:GM1 in the molar ratio 1:1:1:0.2 were classed as the first generation.

Abuchowski et al.⁸¹ were among the first to covalently couple polyethylene glycol (PEG) to a bovine liver catalase, which provided a hydrophilic shield around the enzyme and delayed recognition by the MPS. This method transcended to liposomal modification by PEG and performed better than earlier methods that used glycolipids. This was followed by several publications on superior performance of PEGylated liposomes tested *in vivo* with various drugs.^{62,67,68,82–93} Allen and Hansen demonstrated an elaborate pharmacokinetic performance that was dependent on the dosage effect between the stealth and conventional liposomes; a comparison was also made between the half-lives of first-generation GM1 liposomes and second-generation PEG(1900)-distearoylphosphatidylethanoalamine.^{62,67,85} Gabizon et al. were the first to demonstrate the extended blood lifetime of PEGylated liposomes encapsulating doxorubicin in human subjects.⁸⁸ This was followed

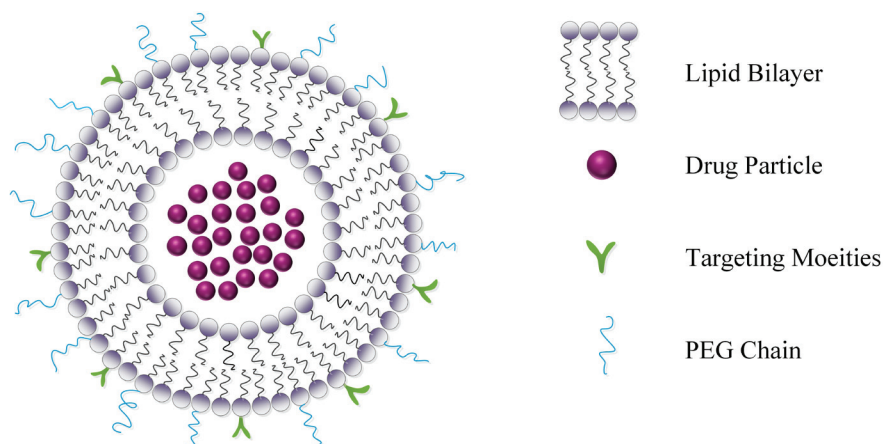


FIG. 2: Schematic of a copolymer liposome structure. The constituent building blocks have a hydrophobic tail and hydrophilic head that self-assemble to form the unique bilayer membrane. The liposomal surface can be conjugated to any functional molecule pertaining to the desired application and PEGylated for increased steric shielding.

by clinical trials of doxorubicin in stealth liposomes on 15 human immunodeficiency virus (HIV)-infected patients for the treatment of Kaposi's sarcoma.⁸⁹ Liposomes modified with PEG were also used as drug carrier devices for gene delivery, specifically for delivery of pDNA⁹⁴ and siRNA.⁹⁵ In 1990, the FDA approved adagen, a polymer–drug conjugate of adenosine deaminase with PEG. This was followed by approval of PEGylated liposomal doxorubicin for cancer treatment in 1995. Many researchers investigated the versatility of PEGylated liposomes for various drug deliveries, including those for cancer, and conclusively established the higher lifetime of PEGylated DDS.^{70,95–110} Compared to first-generation stealth liposomes such as the GM and SM liposomes mentioned above, PEGylated liposomes demonstrated the ability to evade activating the immune system. Gradually, however, several disadvantages were identified and associated with PEGylation in subsequent research, known as the “PEG dilemma.”¹¹¹ Earlier, the pharmacokinetics of PEG liposomes were proven to be independent of dosage unless the quantity administered was too low, at which accelerated blood clearance, abbreviated as the ABC-effect, was observed. This phenomenon occurred after successive bolus injections of liposomes were administered, after a prior sample was already injected.^{71–120} This event is attributed to production of anti-PEG immunoglobulin from spleen in reaction to the prior doses, which increase uptake by Kupffer cells and can be suppressed to some extent by choosing antiproliferative drugs or moieties.³⁷

B. Polymeric Micelles, Polymeric NPs, and Solid Lipid NPs

Micelles (Fig. 3) differ from liposomes in their structure. Liposomes are lipid bilayers (Fig. 2) that separate an internal aqueous phase from an external aqueous environment, whereas polymeric micelles (PM) are lipid monolayers (Fig. 3) with two functional parts: an inner hydrophobic core that determines loading efficiency of desired drugs and an outer hydrophilic shell that controls pharmacokinetic behavior of the micelle *in vivo*.^{39,121,122} The outer polymeric corona acts as a steric shield, camouflaging the drug loaded in the solid inner core, and it can be conjugated to targeting or recognition moieties. They are smaller in size (<100 nm), have superior stealth properties when compared to liposomes, and are created by self-assembly of amphiphilic diblock or triblock copolymeric molecules, which in turn are a mix of hydrophilic and hydrophobic components. Lee et al. showed superior pharmacokinetic properties of polymeric vesicles over stealth liposomes.⁵⁹ This class of DDS has gathered much interest because of their similarity to natural biological transport systems; their unique characteristics delay uptake by RES and facilitate efficient intracellular drug delivery.¹²³

Any amphiphilic biocompatible polymer capable of significant steric hindrance such as PEG and polyvinylpyrrolidone can be used to make micelles.³⁹ A popular class of micelles marketed as Pluronics®, also known under the nonproprietary name of po-

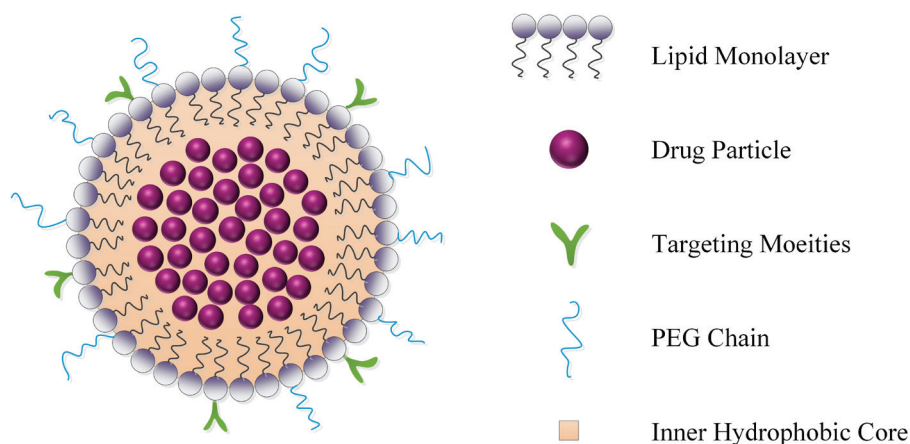


FIG. 3: Schematic of a polymeric micelle/SLN. The inner matrix holds the drug cargo, protected by the outer shell that may be activated by attachment of various molecules.

loxamers, consists of polyethylene oxide (PEO) and polypropylene oxide in an ABA triblock structure. These micelles have relatively longer elimination half-lives than liposomes.¹¹⁴ For instance, P85 was shown to have a half-life of between 60 and 90 h.⁵⁸

Poloxamine (PX) and poloxamer were noticed to impart stealth properties when coated on a drug particle. Illum and Davis were among the first to use them for modification of polystyrene and poly(methyl methacrylate) NP.^{124,125} Uptake by liver was seen to decrease by 20% and 40% for NPs coated with poloxamer-188 and -338, respectively. Poloxamer-407 was seen to perform even better than either in terms of evading phagocytosis, whereas PX proved to be superior over poloxamer.¹²⁶ Rudt and Muller conducted an assay of NP and microparticle pharmacokinetics affecting phagocytosis for polystyrene modified by PX.¹²⁷ Moghimi et al. established that injecting PX-908 caused rapid clearance of a second dosage, most likely by resident macrophages and Kupffer cells present from the previous dose. Such behavior was noticed to be exactly similar to that resulting from coating the particle with PX-908.^{128,129} Modification with other polymers, such as poly(lactic-co-glycolic) acid (PLGA), also resulted in enhanced circulation lifetimes.^{130–132}

PEG has also been widely used as a constituent of diblock and multiblock copolymer micelles that were shown to have longer circulation lifetimes.¹²³ Several stimuli-responsive PM have been designed,¹³³ and some are in final stages of clinical trials.³⁹ Triblock copolymer micelles of ABA and BAB combinations of PEG and poly(lactic) acid (PLA)

were designed and tested as a DDS for paclitaxel in mice.¹³⁴ Moffatt and Cristiano used one such copolymer, PLGA-PEG-PLGA, as a gene delivery vehicle for encapsulated salicylhydroxamic acid-PEI/pDNA.¹³⁵ Various other polymeric NPs were formulated and tested for suitability as a drug carrier. Verrechia et al. modified PLA/albumin to PLA-PEG copolymer and recorded an extended half-life of 6 h more than the former's few minutes.⁶⁹ Zhiqing et al. studied PEGylated PLGA NPs (stealth NPs) as carriers for arsenic trioxide and showed that they had lower uptake by murine peritoneal macrophages compared to that of naked arsenic trioxide.¹³⁶ Bazile et al. developed the methoxy-based NP Me-PEG-PLA and recorded a longer half-life of 6 h, compared to a few minutes for F68-coated NP.¹³⁷ This was followed by other PLA-PEGs complexed with NPs for stealth delivery.^{138,139} In addition, PEGylated PLGA microparticles encapsulating VEGF with improved circulation times was proposed recently.¹⁴⁰

Gref et al. structured NPs with PLA and monomethoxy polyoxyethylene,¹⁴¹ followed by Peracchia et al., who developed coated polycyanoacrylate NPs and poly(isobutyl-2-cyanoacrylate) with PEG. The researchers observed increased circulation time and decreased cytotoxicity.^{142–144} Ahmed and Discher¹⁴⁵ designed PEG-PLA, PEG-polycaprolactone, and PEG-polybutadiene hydrolysis-triggered polymericosomes. PEG was incorporated to improve *in vivo* circulation, and the authors presented a comparison between PEG-polymericosome and stealth liposome. Lee et al. reported a best half-life of 47.3 ± 1.8 h⁵⁹ for polymericosome-10, whereas Photos et al. report-

ed a half-life of 28 ± 10 h for OB16.⁷² Both results were significant improvements over the half-lives of stealth liposomes.

PEO was extensively studied as a prospective drug particle shield. Jaeghere et al. modified NPs with PEO and assayed the factors that determined MPS uptake.¹⁴⁶ Vittaz et al. conducted a similar study with a complex of PLA-PEO and concluded that the decrease in phagocytosis is directly proportional to the surface density of PEO.¹⁴⁷ PLA NPs, when modified into a diblock copolymer by monomethoxypoly(ethylene oxide)-poly(lactic acid), were seen to undergo delayed phagocytosis in guinea pigs.¹⁴⁸ Butsele et al. tested poly(2-vinylpyridine)-PEO-poly(caprolactone) (P2VP-PEO-PCL) triblock copolymer as a pH-triggered drug delivery device and found it to possess stealth behavior.¹⁴⁹ A detailed review of various polymeric coatings and the behavior of complement activation mediated by polymeric structure is provided by Salmaso and Caliceti.¹⁵⁰

NK911 is a micelle with a diameter of 40 nm, constructed from PEG-poly(aspartic acid) block copolymer and encapsulating doxorubicin. NK911 is the first polymeric micelle that was approved for clinical trial on 23 patients with malignant tumors.⁵⁶ PEG formed the outer core, adding the “stealth” characteristic, and the poly(aspartic acid) chain conjugated to doxorubicin built the inner hydrophobic core. The dosage was gradually increased from 6.0 to 67 mg of doxorubicin equivalent/m² in several levels. The half-life for NK911 was observed to be longer than that of free drug. Following this, several other micelle structures were developed that proceeded to human trials.¹⁵¹ Micelles have been conjugated to antibodies, nucleic acids, peptides, and other biomolecules to augment target specificity and localization.

Solid lipid nanoparticles (SLNs), usually characterized as having a solid lipid core, have been proposed as an alternate drug carrier.¹⁵² Following this, Bocca et al.¹⁵³ modified SLNs with dipalmitoylphosphatidylethanolamine-PEG and stearic acid-PEG as stealth agents for fluorescent rhodamine B. Stealth SLNs were noticed to be nonphagocytized after 60 min of administration, compared to phagocytosis of plain SLNs in few minutes. This was followed by the use of stealth SLNs to deliver doxorubicin in rats⁷⁴ and icariin in mice.⁷³ Madan et al. also used PEG NPs to deliver noscapine across the blood-brain barrier to glioblastoma cells.¹⁵⁴

C. Dendrimers

Dendrimers (Fig. 4), a whole new class of drug carriers, were proposed in the 1980s.¹⁵⁵ Since then, these highly branched macromolecules with low polydispersity have been extensively explored as drug carriers. They have garnered much interest as a pharmaceutical vehicle because of their unique structural properties. Dendrimers have a central core that can be loaded with hydrophobic drugs, a branched shell that can impart steric stability, and surface three-dimensional (3D) moieties that can be conjugated with targeting bioactive molecules.¹⁵⁶ Polyamidoamine (PAMAM) dendrimers or Starburst® dendrimers are the most common. These are dendrimers made of poly(lysine), poly(propyleneimine), polyester, polyol, and triazine. PEGylated dendrimers with comparatively longer terminal lifetimes have been also reported.^{75,157,158} It was observed that cationic dendrimers were flushed out of circulation in Wistar rats at higher accelerated rates than anionic dendrimers, which reconfirmed that surface charge is a factor that significantly determines opsonization rate.¹⁵⁸ Detailed pharmacokinetic dependency between dendrimer shape and drug content on its longevity *in vivo* has been studied.^{76,159}

Vivagel™ (Starpharma), an amide-based (SPL7013) dendrimer microbicide, was cleared for clinical trials against herpes simplex virus (HSV) and HIV in 2004.^{160–162} SPL7013 has a core of benzhydrylamine amide of L-lysine bonded to four layers of L-lysine branches, and each of the 32 amine groups on the surface were terminated by a sodium 1-(carboxymethoxy) naphthalene-3,6-disulfonate group. It was suggested that SPL7013 attached itself to gp120 proteins on viral surfaces, and this may have prevented it from adhering to human cells.

D. Polymeric Modifications of Other Substrates

Liu et al. grafted PEG onto single-walled nanotubes (SWNTs) and noticed increased circulation time with increased chain length,¹⁶³ recording 15 h for triple-branched PEG grafted onto SWNTs. Prencipe et al. reported 22.1 h for polyglutamic acid-pyrene-mPEG.¹⁶⁴ Niidome et al. layered gold nanorods with PEG to decrease its cytotoxicity and increase its lifetime, with an objective of photothermal therapy and/or photocontrolled DDS.^{165,166} Yokoyama et al. conjugated the antitumor drug adriamycin (ADR) with

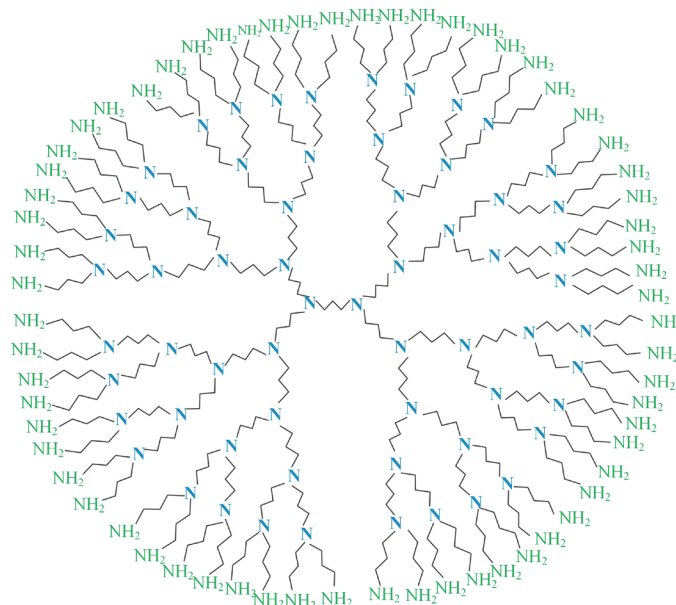


FIG. 4: Schematic of the PAMAM dendrimer. Starting from an initiator core, the branching increases outward in a tree-like structure that is terminated by amine branches. The dendrimer surface can also be conjugated to other molecules by correct protonization.

PEG and showed it to have a longer half-life (70 min) than noncomplexed ADR (18 min).⁶⁰ Zhou et al. used camptothecin (CPT) to form PEG-block-dendritic polylysine-CPT nanospheres/nanorods of different sizes intended for drug delivery to cancerous cells.¹⁶⁷ PEG-tetra-CPT-nanorods with dimensions <500 nm were found to have the longest lifetime and target specificity among all other sized nanorods.

In 1997, Cho et al. proposed a carbohydrate coating of NP that eluded phagocytic tagging by the MPS.¹⁶⁸ In the same year, Maruyama et al. developed a new class of gene carrier with polysaccharide and PLA grafted onto poly(L-lysine).¹⁶⁹ Recently, super paramagnetic iron oxide (SPIO) NPs have been gaining popularity as MRI contrast agents and for treatment of cancer by hyperthermia. However, SPIO is not biocompatible and must be shielded from phagocytosis. SPIO with surface modifications of chitosan,¹⁷⁰ PLA-PEG,¹⁷¹ PEG,¹⁷² and PEG-poly(amino) acid¹⁷³ have been proposed.

III. NATURAL AND SEMINATURAL STEALTH ENGINEERING TECHNIQUES FOR IN VIVO DRUG DELIVERY

Liposomes, PM, SLNs, and dendrimers are artificial DDSs developed in an attempt to extend drug

longevity *in vivo*. However, research has shown that they were still subjected to rapid elimination from the blood. This motivated several researchers to explore natural biological structures as potential DDSs, including erythrocytes and capsids. The following section presents a short review on such developments.

A. Red Blood Cell (Erythrocyte)-Based DDSs

Red blood cells (RBCs; also called erythrocytes) are anucleate cells that transport oxygen and carbon dioxide between lungs and tissues via the circulatory system. In humans, healthy mature RBCs are biconcave shaped, measure $\sim 7.7 \mu\text{m}$ in diameter, and have a lifetime of ~ 120 d. Their cytoplasm contains hemoglobin, a metalloprotein of iron that binds with oxygen. RBCs are found in all vertebrates (except for the family Channichthyidae) and a few invertebrates. The discocytes are biocompatible, abundant, and nontoxic and normally do not instigate the MPS for opsonization. Additionally, their anucleate nature allows a considerably inert intracellular condition and high drug loadability. These aspects make this cell a probable DDS with extended vascular circulation, thereby reducing frequency and intensity of dosage.^{77,174} A common method to insert a load

into an RBC is to degrade it in hypotonic solutions, which is followed by drug absorption and membrane resealing. However, research has shown that this method almost always caused hemolysis, irreversible morphological damage to the RBC structure, and phosphatidyl serine (PS) exposure. PS has been associated with early removal of RBC by the MPS.¹⁷⁵ RBCs can also be loaded by pretreating with chlorpromazine, which causes reversible swelling and endocytosis of payload. In other research, RBC membranes were fused with liposomes containing the therapeutic load, and the liposomes then release it gradually inside the erythrocytic cell.^{175,176} Other common methods are electroporation by exposure to a strong electric field and drug-induced endocytosis.¹⁶⁷ In 2014, He et al. proposed a novel method of loading protein into RBCs by using covalent bonding between the protein and a cell-penetrating peptide (CPP) via a disulfide link.¹⁷⁷ The CPP penetrates the RBC without any membrane disruption. Once inside the RBC, the disulfide bond dissociates, thus successfully enclosing the protein inside the cell and ensuring its structural and functional integrity.

RBCs have surface antigens that react with antibodies present in blood of a different type; this necessitates proper matching during transfusion. To facilitate easy transfusion without cross-matching, shielding the antigens by modifying RBCs with mPEG was first achieved by a group of researchers in 1996.¹⁷⁸ This was soon followed by work of other investigators, some attempting to optimize polymer structure with respect to cytotoxicity.^{179–186} Scott and Chen extended PEGylation to other allogenic and xenogenic cells including white blood cells.¹⁸⁷

Several drugs have also been successfully encapsulated and tested *in vivo*.^{77,174} One of the early clinical studies on nine volunteers using 51Cr-labeled autologous RBC showed a normal *in vivo* half-life of 19–29 d.¹⁸⁸ This was succeeded by another clinical study of PEG-conjugated adenosine deaminase (pegademase) and native adenosine deaminase (ADA)-loaded 51Cr-labeled RBC by hypo-osmotic dialysis. A half-life of 20 d and 12.5 d was reported for erythrocyte-entrapped pegademase and ADA, respectively, compared to 3–6 d of exposed pegademase.¹⁸⁹ Chambers and Mitragotri attempted noncovalent binding of 200–450-nm polystyrene NPs to RBC membrane, which were injected in Sprague-Dawley rats. Results showed an increment in circulation time for the RBC NPs; ~5% were

still circulating after 12 h, whereas >99.9 % of unbound particles cleared in 2 min.¹⁹⁰ In a clinical trial to evaluate potency of low doses of corticosteroid in cystic fibrosis patients, autologous erythrocytes were loaded with dexamethasone 21-phosphate and administered to 17 subjects in two phases during a time interval. Although no side effects or toxicity were recorded, a persistent level of dexamethasone was detected in plasma for at least up to 10 d after injection, proving efficacy of these low dexamethasone doses over standard direct therapeutic dosage.¹⁹¹ Amikacin, an aminoglycoside antibiotic, was encapsulated in RBCs for protection against enzymatic degradation and then targeted to peritoneal macrophages in rats. The study revealed a significant improvement in pharmacokinetics of the antibiotic, with more than a fivefold increase in half-life of enclosed drug over free drug.^{192,193} Phenylalanine hydroxylase (PAH), an enzyme that initiates and controls processing of phenylalanine, is an essential amino acid; a deficiency can cause phenylketonuria. To find a sustained alternate enzyme replacement therapy for PAH, Yew et al. enclosed PAH in RBCs by hypotonic dialysis and then injected the drug into mice. A persistent level of PAH remained in circulation for at least 10 d, along with a decrease in phenylalanine levels by 80%.¹⁹⁴ Chitosan is another popular colloidal drug delivery substrate; however as an intravascular DDS, it becomes flushed out from circulation easily. To extend its lifetime, low-molecular-weight chitosan was attached onto RBC surface by electrostatic attraction and the combination was demonstrated to be a feasible DDS.¹⁹⁵ Among several such therapeutic molecules enclosed in RBCs are immunophilin,¹⁹⁶ paclitaxel,¹⁹⁷ bovine serum albumin,¹⁹⁸ piperine,¹⁹⁹ and IFN α 2b.²⁰⁰ Apart from their use with drugs, RBCs have also been used to encapsulate gold NPs to facilitate high contrast in dynamic X-ray imaging,²⁰¹ which indicates the flexibility and lucrativeness of RBCs as a functional DDS.

B. Viral Capsid DDSs

Viruses are submicroscopic parasitic agents that are characterized by an RNA/DNA core that is encapsulated by a protein coat. They can effortlessly penetrate living cells and cause unwanted effects, such as infection or mutation. However, because of this same property, platforms derived from viral sources

have been evaluated for possible DDSs.²⁰² A capsid is the outer shell of a virus composed of protein subunits called capsomeres. The viral genetic material can be extracted and then substituted by the desired load, and the capsid is then reassembled.²⁰² Such a process prevents the capsid from replicating and infecting the host, but still retains their MPS-evasive properties. Viral vectors are slowly gaining preference as carrier of transgenes for gene therapy, because they enable efficient transfer and sustained gene expression. Cooper and Shaul used hepatitis B viral capsid to enclose oligonucleotides (ONs). They first permeabilized the virus and treated it with ribonuclease, causing evacuation of endogenous RNA. This process was followed by incubation with ONs and capsid restructuring, which successfully encapsidated the ONs.²⁰³ These investigators also tested the particles on cultured HeLa cells and observed a higher cell uptake than that of naked ONs and as well as a lack of cytotoxicity, providing proof of ONs as a viable DDS. Adeno-associated viral (AAV) serotypes were obtained by transfection of 293T cells.²⁰⁴ AAV was then injected into neonatal mice brain at delivery, and the mice were sacrificed after 30 d. An examination of the brain sections affirmed efficient transduction. AAV serotypes have also been used to provide a medium for conjugation and delivery of paclitaxel.²⁰⁵ This process could eliminate the potential virulence of chemical solvents currently used to deliver paclitaxel, which has low water solubility. In a thorough review by Selvam et al.,²⁰⁶ several viral vectors were modified for gene transportation in lacrimal glands.

Plant viruses, which are expected to be less pathogenic and immunostimulatory than animal viruses, were used to show viability as DDSs. A group of investigators encapsulated doxorubicin in hibiscus chlorotic ringspot virus and targeted it to an ovarian cancer cell line, observing a statistically higher uptake and cytotoxicity in cancer cells.²⁰⁷ Cucumber mosaic virus was also loaded with doxorubicin and conjugated with folic acid as a targeting moiety.²⁰⁸ The combination was tested both *in vitro* and *in vivo* and exhibited enhanced antitumor action and reduced cardiotoxicity.

C. DNA-Based Drug Delivery Systems

The quest to develop an ideal DDS that avoids opsonization and renal flushing by MPS recognition

as a native molecule has seen the design of a novel group of delivery structures based on the endogenous structure of DNA. DNA is a biopolymer that encodes genetic information that is uniquely characterized to every living organism. It is inherently biocompatible, biodegradable, and physiologically stable and has engaged much interest during the past few years as a possibility for an efficient DDS.²⁰⁹ DNA consists of two polynucleotide strands coiled helically. Each nucleotide in a strand is constructed from either one from purine base (adenine, guanine) or one pyrimidine base (cytosine, thymine) on a deoxyribose sugar and phosphate backbone. The phosphate of one nucleotide covalently binds to the sugar of an adjoining nucleotide, and its nitrogenous base forms a pair with the base of the other strand, together also known as base pairs. Base pairs can only be formed between adenine and guanine or cytosine and thymine, and this is commonly termed complementary base pairing.

The famous DNA “origami” technique proposed by Paul Rothemund²¹⁰ is contingent on the unique base-pairing feature of DNA (Fig. 5a). Rothemund manipulated DNA strands using short complementary synthetic ON staples to assemble various shapes and patterns, such as a smiley face, map of China/North America, and stars. Lo and coworkers were the first to use DNA origami to create 3D structures, followed by other research groups.²¹¹ To deliver Cy3 to cancer cells, Ko et al. used 52-base-long single-stranded DNA with four palindrome segments to self-assemble into DNA-NTs of length 50–200 nm and a diameter of 40 μm .²¹² Bhatia et al. described the potential of these nanostructures for cargo delivery by designing DNA icosahedra using a modular assembly approach and encapsulating with gold NPs (Fig. 4).²¹³ These structures are suitable for drug delivery because they have a high capacity to carry drug as well as a well-defined structure, biocompatibility, stability in physiological environment, and commendable half-lives.²¹⁴ Two-dimensional triangular and 3D tubular origami structures were independently loaded with doxorubicin by intercalation and exposed to regular and doxorubicin-resistant human adenocarcinoma breast cells (MC7).²¹⁵ Although the DNA nanostructures by themselves were noncytotoxic to the cell line, those loaded with drug induced cell death in both types of MC7; free doxorubicin was ineffective against the resistant type. Another group conjugated DNA tetrahedron with doxorubi-

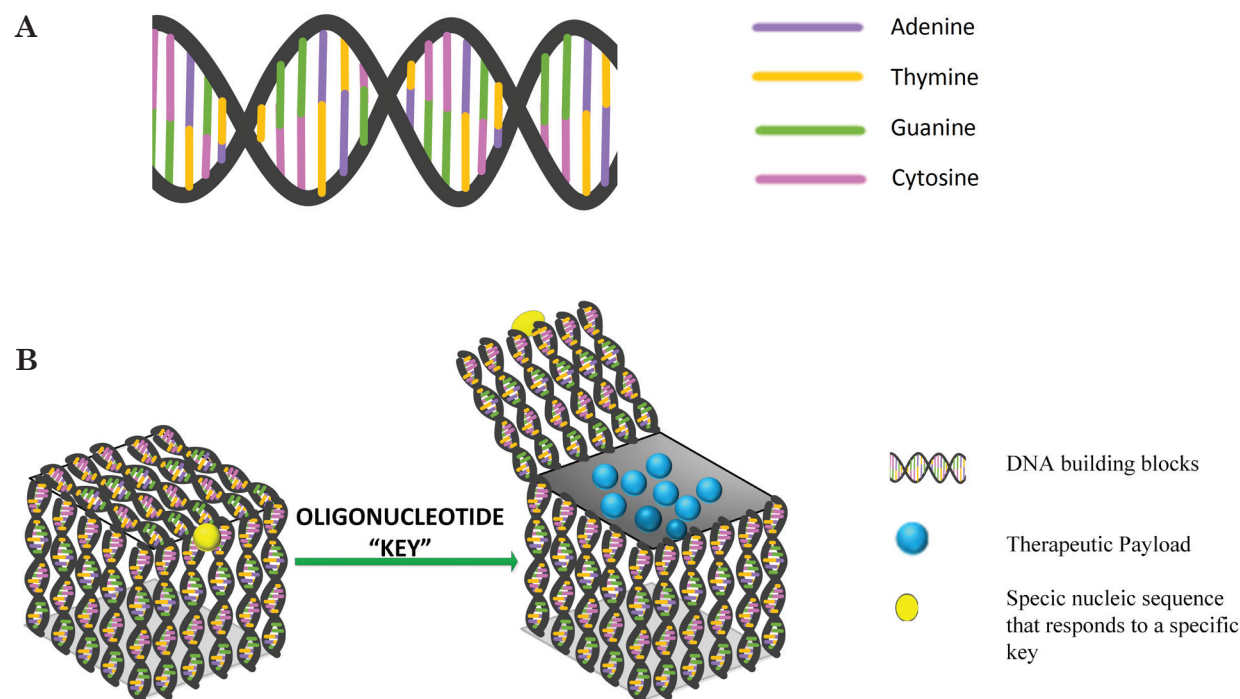


FIG. 5: (a) Structure of DNA shows Watson–Crick complementary pairing. Adenine can bond only with thymine and guanine with cytosine. (b) The DNA box can ideally be used to store drug molecules until the lid is opened by an ON chain, complementary to the “lock.”

cin and tested it on both receptive and resistive MC7 cell lines. They obtained similar results, confirming that DNA nanostructures had an enhanced intracellular uptake and were thus capable of reversing drug resistivity.²¹⁶ Chang et al. incorporated doxorubicin in DNA-icosahedra (Doxo@DNA-icosa) and aptamer-conjugated DNA-icosahedra (Doxo@Apt-DNA-icosa) and then exposed the drug to MUC-1-negative Chinese hamster ovary cell (CHO-K1) and MUC1-positive human breast cancer cell (MCF-7) cultures.²¹⁷

Doxo@Apt-DNA-icosa showed a higher intracellular absorption in MCF-7 but not in CHO-K1 cells. Doxo@DNA-icosa had greater cell lethality to MCF-7 when compared with free doxorubicin and Doxo@DNA-icosa. These data indicate the possibility of an efficient targeted DDS. Choi et al. formulated a cancer-cell-targeting DNA hybrid duplex of DNA-cholesterol and DNA-peptide that self-assembled into liposomal NPs in solution.²¹⁸ The duplex was then loaded with doxorubicin. These NPs released drug at acidic pH, thus demonstrating their capability of functioning as a controllable smart drug. Another research group loaded a similar DNA

complex with curcumin and docetaxel at a high loading efficiency and studied its cytotoxicity against the human lung cancer cell line A549.²¹⁹

Chitosan, another biocompatible polymer sourced from chitin, was paired with DNA and doxorubicin as a nanocomplex and had an extended half-life when compared to naked DOX. Its efficacy was also verified against various cell lines.²²⁰ Rolling circle amplification (RCA) is an isothermal process that generates very long periodically sequenced single-stranded DNA. DNA nanoribbons and a few staple ONs were fabricated by RCA.²²¹ They were then coupled with CpG oligodeoxynucleotides as a model drug to prove functionality as a viable DDS. DNA hydrogels composed of CpG DNA were used to deliver doxorubicin and CpG motifs.²²² Andersen et al. proposed an advanced delivery system in which they designed a “DNA box” of dimensions $42 \times 36 \times 36 \text{ nm}^3$ that could only be opened by a matching ON “key”²²³ (Fig. 5b).

IV. CONCLUSIONS

Stealth engineering for DDSs to prolong circulation time and maintain therapeutic levels of drugs in

blood by camouflaging the substrate from the MPS has been a topic of interest for the past 50 years. From surface PEGylation to designing DNA boxes, there have been many optimistic attempts to create the perfect DDS. This review describes the progression of engineering techniques used for DDS and the key results from *in vitro*, *in vivo*, and clinical studies. Such research has many therapeutic applications for humans, including systemic cancer treatment, bone regeneration, gene therapy, pathogenic infection treatment, and insulin control. It has allowed initiation of advanced research in several vistas, such as completely controllable drug delivery, where the dose intensity, duration, and instant can be precisely monitored. An exponential growth of such smart DDSs can be predicted.

REFERENCES

- Gordon S, Taylor PR. Monocyte and macrophage heterogeneity. *Nat Rev Immunol*. 2005 Dec;5(12):953–64.
- Mosser DM, Edwards JP. Exploring the full spectrum of macrophage activation. *Nat Rev Immunol*. 2008 Dec;8(12):958–69.
- Nich C, Takakubo Y, Pajarinen J, Ainola M, Salem A, Sillat T, Rao AJ, Raska M, Tamaki Y, Takagi M, Kontinen YT, Goodman SB, Gallo J. Macrophages-Key cells in the response to wear debris from joint replacements. *J Biomed Mater Res A*. 2013 Oct;101(10):3033–45.
- Kono H, Rock KL. How dying cells alert the immune system to danger. *Nat Rev Immunol*. 2008 Apr;8(4):279–89.
- Zhang X, Mosser DM. Macrophage activation by endogenous danger signals. *J Pathol*. 2008 Jan;214(2):161–78.
- Nathan C. Metchnikoff's legacy in 2008. *Nat Immunol*. 2008 Jul;9(7):695–8.
- Mackaness GB. Cellular immunity and the parasite. *Adv Exp Med Biol*. 1977;93:65–73.
- Dale DC, Boxer L, Liles WC. The phagocytes: neutrophils and monocytes. *Blood*. 2008 Aug;112(4):935–45.
- Chen CJ, Kono H, Golenbock D, Reed G, Akira S, Rock KL. Identification of a key pathway required for the sterile inflammatory response triggered by dying cells. *Nat Med*. 2007 Jun;13(7):851–6.
- Park JS, Svetkauskaite D, He Q, Kim JY, Strassheim D, Ishizaka A, Abraham E. Involvement of Toll-like receptors 2 and 4 in cellular activation by high mobility group box 1 protein. *J Biol Chem*. 2004 Dec;279(9):7370–7.
- Akira S. Toll-like receptor signaling. *J Biol Chem*. 2003 Oct;278(40):38105–8.
- Doyle SL, O'Neill LAJ. Toll-like receptors: From the discovery of NF- κ B to new insights into transcriptional regulations in innate immunity. *Biochem Pharmacol*. 2006 Oct;72(9):1102–13.
- Duerst R, Werberig K. Cells of the J774 macrophage cell line are primed for antibody-dependent cell-mediated cytotoxicity following exposure to gamma-irradiation. *Cell Immunol*. 1991 Sept;136(2):361–72.
- Lambert LE, Paulnock DM. Modulation of macrophage function by gamma-irradiation-Acquisition of the primed cell intermediate stage of the macrophage tumoricidal activation pathway. *J Immunol*. 1987 Oct;139(8):2834–41.
- Carozzi S, Caviglia PM, Nasini MG, Schelotto C, Santoni O, Pietrucci A. Peritoneal dialysis solution pH and Ca²⁺ concentration regulate peritoneal macrophage and mesothelial cell activation. *Asaio J*. 1994 Jan-Mar;40(1):20–3.
- Pabst MJ, Pabst KM, Handsman DB, Beranova-Giorgianni S, Giorgianni F. Proteome of monocyte priming by lipopolysaccharide, including changes in interleukin-1 β and leukocyte elastase inhibitor. *Proteome Sci*. 2008 May;6(13).
- Tang L, Hu W. Molecular determinants of biocompatibility. *Expert Rev Med Devices*. 2005 Jul;2(4):493–500.
- Peters-Golden M. Putting on the brakes: Cyclic AMP as a multipronged controller of macrophage function. *Sci Signal*. 2009 Jun;2(75):pe37.
- Wall EA, Zavzavadjian JR, Chang MS, Randhawa B, Zhu X, Hsueh RC, Liu J, Driver A, Bao XR, Sternweis PC, Simon MI, Fraser ID. Suppression of LPS-induced TNF- α production in macrophages by cAMP is mediated by PKA-AKAP95. *Sci Signal*. 2009 Jun;2(75):ra28.
- Ham EA, Soderman DD, Zanetti ME, Dougherty HW, McCauley E, Kuehl FA. Inhibition by prostaglandins of leukotriene B₄ release from activated neutrophils. *Proc Natl Acad Sci USA*. 1983 Jul;80(14):4349–53.
- Harizi H, Juzan M, Pitard V, Moreau JF, Gualde N. Cyclooxygenase-2-issued prostaglandin E₂ enhances the production of endogenous IL-10, which down-regulates dendritic cell functions. *J Immunol*. 2002 Mar;168(5):2255–63.
- Diaz A, Varga J, Jimenez SA. Transforming growth factor-beta stimulation of lung fibroblast prostaglandin E₂ production. *J Biol Chem*. 1989 Jul;264(20):11554–7.
- Kohyama T, Liu X, Kim HJ, Kobayashi T, Ertl RF, Wen FQ, Takizawa H, Rennard SI. Prostacyclin analogs inhibit fibroblast migration. *Am J Physiol Lung Cell Mol Physiol*. 2002 Aug;283(2):L428–32.
- Bangham AD, Standish MM, Watkins JC. Diffusion of univalent ions across the lamellae of swollen phospholipids. *J Mol Biol*. 1965 Aug;13(1):238–52.
- Gregoriadis G. Liposomes In Drug Delivery: Present and Future. *Liposome Dermatics*. 1992;346–52.
- Gregoriadis G, Ryman BE. Liposomes as carrier of enzymes or drugs: a new approach to the treatment of storage diseases. *Biochem J*. 1971 Oct;124(5):58.
- Segal AW, Gregoriadis G, Black CDV. Liposomes as vehicles for local release of drugs. *Clin Sci Mol Med*. 1975 Aug;49(2):99–106.
- Gregoriadis G. The carrier potential of liposomes in biology and medicine (first of two parts). *N Engl J Med*. 1976 Sep;295(14):704–10.
- Gregoriadis G. The carrier potential of liposomes in biology and medicine (second of two parts). *N Engl J Med*. 1976 Sep;295(14):765–70.

30. Gregoriadis G. Drug Entrapment in Liposomes. *FEBS Lett.* 1973 Nov;36(3):292–6.
31. Gregoriadis G, Putman D, Louis L, Neerunjun D. Comparative effect and fate of non-entrapped and liposome-entrapped neuraminidase injected into rats. *Biochem J.* 1974 May;140(2):323–30.
32. Allen TM, Cullis PR. Liposomal Drug Delivery Systems: From concept to clinical applications. *Adv Drug Deliv Rev.* 2013 Jan;65(1):36–48.
33. Hoekstra D, Scherphof C. Effect of fetal calf serum and serum protein fractions on the uptake of liposomal phosphatidylcholine by rat hepatocytes in primary monolayer culture. *Biochim Biophys Acta.* 1979 Feb;551(1):109–121.
34. Chonn A, Semple SC, Cullis PR. Association of blood proteins with large unilamellar liposomes in vivo (Relation to circulation lifetimes). *J Biol Chem.* 1992 Sep;267(26):18759–65.
35. Stolnik S, Illum L, Davis SS. Long circulating microparticle drug carriers. *Adv Drug Deliv Rev.* 1995 Sep;16(2-3):195–214.
36. Yoo J, Doshi N, Mitragotri S. Adaptive micro and nanoparticles: Temporal control over carrier properties to facilitate drug delivery. *Adv Drug Del Rev.* 2011 Nov;63(14-15):1247–56.
37. Yamashita F, Hashida M. Pharmacokinetic considerations for targeted drug delivery. *Adv Drug Del Rev.* 2013 Jan;65(1):139–47.
38. Torchilin VP, Trubetskoy VS. Which polymers can make nanoparticulate drug carriers long-circulating?. *Adv Drug Deliv Rev.* 1995 Sep;16(2-3):141–55.
39. Gong J, Chen M, Zheng Y, Wang S, Wang Y. Polymeric micelles drug delivery system in oncology. *J Control Release.* 2012 May;159(3):312–23.
40. Venkataraman S, Hedrick JL, Ong ZY, Yang C, Ee PLR, Hammond PT, Yang YY. The effects of polymeric nanostructure shape on drug delivery. *Adv Drug Del Rev.* 2011 Nov;63(14-15):1228–46.
41. Geng Y, Dalhaimer P, Cai S, Tsai R, Tewari M, Minko T, Discher DE. Shape effects of filaments versus spherical particles in flow and drug delivery. *Nat Nanotechnol.* 2007 Apr;2(4):249–55.
42. Champion JA, Mitragotri S. Shape induced inhibition of phagocytosis of polymer particles. *Pharm Res* 2009 Apr;26(1):244–9.
43. Abra RM, Bosworth ME, Hunt CA. Liposome Deposition in vivo: effects of pre-dosing with liposomes. *Res Commun Chem Pathol Pharmacol.* 1980 Aug;29(2):349–60.
44. Kao YJ, Juliano KL. Interactions of liposomes with reticuloendothelial system. Effects of reticuloendothelial blockade on clearance of large unilamellar vesicles. *Biochim Biophys Acta.* 1981 Nov;677(3-4):453–61.
45. Abra RM, Hunt CA. Liposome Disposition in vivo III: Dose and vesicle size effects. *Biochim Biophys Acta.* 1981 Dec;666(3):493–503.
46. Abra RM, Hunt CA. Liposome disposition in vivo IV: the interaction of sequential doses of liposomes having different diameters. *Res Commun Chem Pathol Pharmacol.* 1982 Apr;6(1):17–31.
47. Bradfield JWB, Souhami RL, Addison IE. Mechanism of adjuvant effect of dextran sulphate. *Immunology.* 1974 Feb;26(2):383–92.
48. L'Age-Stehr J, Diamantstein T. Suppression and potentiation of expression of delayed type hypersensitivity by dextran sulphate. *Immunology.* 1977 Aug;33(2):179–83.
49. Patel KR, Li MP, Baldeschwieler JD. Suppression of liver uptake of liposomes by dextran sulphate 500. *Proc Natl Acad Sci. USA.* 1983 Nov;80(21):6518–22.
50. Aragnol D, Leserman LD. Immune Clearance of Liposomes inhibited by an anti-Fc receptor antibody in vivo. *Proc Natl Acad Sci. USA.* 1986 Apr;83(8):2699–703.
51. Toutain PL, Bousquet-Melou A. Plasma terminal half-life. *J vet Pharmacol Ther.* 2004 Dec;27(6):427–39.
52. Zhang Y, Chan HF, Leong KW. Advanced materials and processing for drug delivery: The past and the future. *Adv Drug Deliv Rev.* 2013 Oct;65(1):104–20.
53. Kim TY, Kim DW, Chung JY, Shin SG, Kim SC, Heo DS, Kim NK, Bang YJ. Phase I and pharmacokinetic study of genexol-PM, a cremophor-free, polymeric micelle-formulated paclitaxel, in patients with advanced malignancies. *Clin Cancer Res.* 2004;10:3708–16.
54. Hamaguchi T, Matsumura Y, Suzuki M, Shimizu K, Goda R, Nakamura I, Nakatomi I, Yokoyama M, Kataoka K, Kakizoe T. NK105, a paclitaxel-incorporating micellar nanoparticle formulation, can extend in vivo antitumour activity and reduce the neurotoxicity of paclitaxel. *Br J Cancer.* 2005;92:1240–6.
55. Uchino H, Matsumura Y, Negishi T, Koizumi F, Hayashi T, Honda T, Nishiyama N, Kataoka K, Naito S, Kakizoe T. Cisplatin-incorporating polymeric micelles (NC-6004) can reduce nephrotoxicity and neurotoxicity of cisplatin in rats. *Br J Cancer.* 2005;93:678–87.
56. Matsumura Y, Hamaguchi T, Ura T, Muro K, Yamada Y, Shimada Y, Shirao K, Okusaka T, Ueno H, Ikeda M, Watanabe N. Phase I clinical trial and pharmacokinetic evaluation of NK911, a micelle encapsulated doxorubicin. *Br J Cancer.* 2004;91:1775–81.
57. Danson S, Ferry D, Alakhov V, Margison J, Kerr D, Jowle D, Brampton M, Halbert G, Ranson M. Phase I dose escalation and pharmacokinetic study of pluronic polymer-bound doxorubicin (SP1049C) in patients with advanced cancer. *Br J Cancer.* 2004;90:2085–91.
58. Batrakova EV, Li S, Li Y, Alakhov VY, Elmquist WF, Kabanov AV. Distribution kinetics of a micelle-forming block copolymer Pluronic P85. *J Control Release.* 2004;100:389–97.
59. Lee JS, Ankone M, Pieters E, Schiffelers RM, Hennink WE, Feijen J. Circulation kinetics and biodistribution of dual-labeled polyerosomes with modulated surface charge in tumor-bearing mice : comparison with stealth liposomes. *J Control Release.* 2011;155:282–8.
60. Yokoyama M, Okano T, Sakurai Y, Ekimoto H, Shibazaki C, Kataoka K. Toxicity and antitumour activity against solid tumours of micelle forming polymeric anticancer drug and its extremely long circulation in blood. *Cancer Res.* 1991;51:3229–36.
61. Peer D, Margalit R. Tumor-targeted hyaluronannano liposomes increase the antitumour activity of liposomal

- doxorubicin in syngeneic and human xenograft mouse tumor models. *Neoplasia*. 2004;6(4):343–53.
62. Allen TM, Mehra T, Hansen C. Stealth Liposomes: An improved sustained release system for 1- β -D-Arabinofuranosyl cytosine. *Cancer Res*. 1992;52:2431–9.
 63. Kirby C, Clarke J, Gregoriadis G. Effect of the cholesterol content of small unilamellar liposomes on their stability in vivo and in vitro. *Biochem J*. 1980 Feb;186(2):591–8.
 64. Gregoriadis G, Davis C. Stability of Liposomes in vivo and in vitro is promoted by their cholesterol content and presence of blood cells. *Biochem Biophys Res Commun*. 1979 Aug;89(4):1287–93.
 65. Semple SC, Chonn A, Cullis PR. Influence of Cholesterol on the association of plasma proteins with liposomes. *Biochemistry*. 1996 Feb;35(8):2521–5.
 66. Begum MY, Abbulu K, Sudhakar M. Flurbiprofen-Loaded stealth liposomes: studies on the development, characterization, pharmacokinetics and biodistribution. *J Young Pharmacists*. 2012 Oct;4(4):209–19.
 67. Chang CW, Barber L, Ouyang C, Masin D, Bally MB, Madden TD. Plasma clearance, biodistribution and therapeutic properties of mitoxantrone encapsulated in conventional and sterically stabilized liposomes after intravenous administration in BDF1 mice. *Br J Cancer*. 1997;75(2):169–77.
 68. Li X, Ding L, Xu Y, Wang Y, Ping Q. Targeted delivery of doxorubicin using stealth liposomes modified with transferrin. *Int J Pharm*. 2009;373:116–23.
 69. Verrecchia T, Spenlehauer G, Bazile DV, Murry-Brelier A, Archimbaud YA, Veillard M. Non-stealth (poly(lactic acid) albumin)) and stealth (poly(lactic acid-polyethylene glycol)) nanoparticles as injectable drug carriers. *J Control Release*. 1995;36:49–61.
 70. Singh M, Ferdous AJ, Kannikkannan N, Faulkner G. Stealth monensin immunoliposomes as potentiators of immunotoxins in vitro. *Eur J Pharm Biopharm*. 2001;52:13–20.
 71. Laverman P, Brouwers AH, Dams CTM, Oyen WJG, Storm G, Rooijen NV, Corstens FHM, Boerman OC. Preclinical and clinical evidence for disappearance of long-circulating characteristics of polyethylene glycol liposomes at low lipid dose. *J Pharmacol Exp Ther*. 2000;293:996–1001.
 72. Photos P, Bacakova L, Discher B, Bates FS, Discher DE. Polymer vesicles in vivo: correlations with PEG molecular weight. *J Control Release*. 2003;90(3):323–34.
 73. Liu K, Wang L, Li Y, Yang B, Du C, Wang Y. Preparation. Pharmacokinetics and tissue distribution properties of icariin-loaded stealth solid lipid nanoparticles in mice. *Chin Herb Med*. 2012;4(2):170–4.
 74. Fundaro A, Cavalli R, Bargoni A, Vighetto D, Zara GP, Gasco MR. Non-stealth and stealth solid lipid nanoparticles (SLN) carrying doxorubicin: pharmacokinetics and tissue distribution after i.v. administration to rats. *Pharmacol Res*. 2000;42(4):337–43.
 75. Kaminskis LM, McLeod VM, Kelly BD, Sberna G, Boyd BJ, Williamson M, Owen DJ, Porter CJH. A comparison of changes to doxorubicin pharmacokinetics, antitumor activity and toxicity mediated by PEGylated dendrimer and PEGylated liposome drug delivery systems. *Nano-med*. 2010;8:103–11.
 76. Zhou Z, Ma X, Jin E, Tang J, Sui M, Shen Y, Kirk EAV, Murdoch WJ, Radosz M. Linear-dendritic drug conjugates forming long-circulating nanorods for cancer drug delivery. *Biomaterials*. 2013;34(22):1–14.
 77. Millan CG, Marinero MLS, Castaneda AZ, Lanao JM. Drug, enzyme and peptide delivery using erythrocytes as carriers. *J Control Release*. 2004;95:27–49.
 78. Gabizon A, Papahadjopoulos D. Liposome Formulations with prolonged circulation time in blood and enhanced uptake by tumors. *Proc Natl Acad Sci USA*. 1988 Sep;85(18):6949–53.
 79. Allen TM, Chonn A. Large unilamellar liposomes with low uptake into the reticuloendothelial system. *FEBS Lett*. 1987 Oct;223(1):42–6.
 80. Allen TM. Stealth Liposomes : avoiding reticuloendothelial uptake. *UCLA symposium in Molecular and Cellular Biology*. 1989;405–15.
 81. Abuchowski A, McCoy JR, Palczuk NC, Es TV, Davis FF. Effect of covalent attachment of polyethylene glycol on immunogenicity and circulating life of bovine liver catalase. *J Biol Chem*. 1977 Jun;25(11):3582–6.
 82. Blume G, Cevc G. Liposomes for the sustained drug release in vivo. *Biochim Biophys Acta*. 1990 Nov;1029(1):91–7.
 83. Klivanov AL, Maruyama K, Torchilin VP, Huang L. Amphipathic polyethylene glycol effectively prolong the circulation time of liposomes. *FEBS Lett*. 1990 Jul;268(1):235–7.
 84. Senior J, Delgado C, Fisher D, Tilcock C, Gregoriadis G. Influence of surface hydrophilicity of liposomes on their interaction with plasma protein and clearance from the circulation: studies with poly(ethylene glycol) coated vesicles. *Biochim Biophys Acta*. 1991 Feb;1062(1):77–82.
 85. Allen TM, Hansen C. Pharmacokinetics of stealth versus conventional liposomes: effect of dose. *Biochim Biophys Acta*. 1991;1068:133–41.
 86. Maruyama K, Yuda T, Okamoto A, Kojima S, Suginata A, Iwatsuru M. Prolonged circulation time in vivo of large unilamellar liposomes composed of distearoylphosphatidylcholine and cholesterol containing amphipathic poly(ethylene glycol). *Biochim Biophys Acta*. 1992;1128(1):44–9.
 87. Woodle MC, Storm G, Newman MS, Jekot JJ, Collins LR, Martin FJ, Szoka FJ. Prolonged systemic delivery of peptide drugs by long circulating liposomes: Illustration with Vasopressin in the Brattleboro rat. *Pharma Res*. 1992;9(2):260–5.
 88. Gabizon A, Catane R, Uziely B, Kaufman B, Safra T, Cohem R, Martin F, Huang A, Barenholz Y. Prolonged circulation time and enhanced accumulation in malignant exudates of doxorubicin encapsulated in polyethylene-glycol coated liposomes. *Cancer Res*. 1994;54(4):987–92.
 89. James ND, Coker RJ, Tomlinson D, Harris JR, Gompels M, Pinching AJ, Stewart JS. Liposomal doxorubicin (doxil): an effective new treatment for Kaposi's sarcoma in AIDS. *Clin Oncol (R Coll Radiol)*. 1994;6(5):294–6.
 90. Vaage J, Donovan D, Uster P, Working P. Tumour uptake

- of doxorubin in polyethylene glycol-coated liposomes and therapeutic effect against a xenografted human pancreatic carcinoma. *Br J Cancer*. 1997;75(4):482–6.
91. Deol P, Khuller GK. Lung specific stealth liposomes: stability, biodistribution and toxicity of liposomal antitubercular drugs in mice. *Biochim Biophys Acta*. 1997;1334:161–72.
 92. Etzerodt A, Maniecki MB, Graversen JH, Moller HJ, Torchilin VP, Moestrup SK. Efficient intracellular drug targeting of macrophages using stealth liposomes directed to the hemoglobin scavenger receptor CD163. *J Control Release*. 2012;160:72–80.
 93. Timo LL, ten Hagen LM, Hossann M, Suss R, van Rhooen GC, Eggermont AMM, Hammerich D, Koning GA. Mild hyperthermia triggered doxorubicin release from optimized stealth thermosensitive liposomes improves intratumoral drug delivery and efficacy. *J Control Release*. 2013;168:142–50.
 94. He ZY, Zheng X, Wu XH, Song XR, He G, Wu WF, Yu S, Mao SJ, Wei YQ. Development of glycyrrhetinic acid-modified stealth cationic liposomes for gene delivery. *Int J Pharm*. 2010;397:147–54.
 95. Herrington TP, Altin JG. Convenient targeting of stealth si RNA-lipoplexes to cells with chelator lipid-anchored molecules. *J Control Release*. 2009;139:229–38.
 96. Namiki Y, Namiki T, Date M, Yanagihira K, Yashiro M, Takahashi H. Enhanced photodynamic antitumor effect on gastric cancer by a novel photosensitive stealth liposome. *Pharmacol Res*. 2004;50:65–76.
 97. Dai W, Yang T, Wang Y, Wang X, Wang J, Zhang X, Zhang Q. Peptide PHSCNK as an integrin $\alpha 5 \beta 1$ antagonist targets stealth liposomes to integrin-overexpressing melanoma. *J Nanomed Nanotechnol*. 2012;8:1152–61.
 98. Ducat E, Deprez J, Gillet A, Noel A, Evrard B, Peulen O, Piel G. Nuclear delivery of a therapeutic peptide by long circulating pH-sensitive liposomes : Benefits over classical vesicles. *Int J Pharm*. 2011;420:319–32.
 99. Gabizon A, Goren D, Horowitz AT, Tzemach D, Losos A, Siegal T. Long-circulating liposomes for drug delivery in cancer therapy: a review of biodistribution studies in tumor bearing animals. *Adv Drug Deliv Rev*. 1997;24:337–44.
 100. Yanagie H, Maruyama K, Takizawa T, Ishida O, Ogura K, Matsumoto T, Sakurai Y, Kobayashi T, Shinohara A, Rant J, Skvarc J, Illic R, Kuhne G, Chiba M, Furuya Y, Sugiyama H, Hisa T, Ono K, Kobayashi H, Eriguchi M. Application of boron-entrapped stealth liposomes to inhibition of growth of tumor cells in the in vivo boron neutron-capture therapy model. *Biomed Pharmacother*. 2006;60:43–50.
 101. Doi AV, Ishiwata H, Miyajima K. Binding and uptake of liposomes containing a poly (ethylene glycol) derivative of cholesterol (stealth liposomes) by the macrophage cell line J774: influence of PEG content and its molecular weight. *Biochim Biophys Acta*. 1996;1278:19–28.
 102. Ranson MR, Cheeseman S, White S, Margison J. Caelyx (stealth liposomal doxorubicin) in the treatment of advanced breast cancer. *Crit Rev Oncol Hematol*. 2001;37:115–20.
 103. Allen TM, Moase EH. Therapeutic opportunities for targeted liposomal drug delivery. *Adv Drug Deliv Rev*. 1996;21:117–33.
 104. Jorgensen K, Davidsen J, Mouritsen OG. Biophysical mechanisms of phospholipase A2 activation and their use in liposome-based drug delivery. *FEBS Lett*. 2002;531:23–7.
 105. Junior A, Mota LG, Nunan EA, Wainstein AJA, Wainstein APDL, Leal AS, Cardoso VN, De Oliveira MC. Tissue distribution evaluation of stealth pH-sensitive liposomal cisplatin versus free cisplatin in Ehrlich tumor-bearing mice. *Life Sci*. 2007;80:659–64.
 106. Timo LL, Hagen LM, Schipper D, Wijnberg TM, van Rhooen GC, Eggermont AMM, Lindner LH, Koning GA. Triggered content release from optimized stealth thermosensitive liposomes using mild hyperthermia. *J Control Release*. 2010;143:274–9.
 107. Li R, Ying X, Zhang Y, Ju R, Wang X, Yao H, Men Y, Tian W, Yu Y, Zhang L, Huang R, Lu W. All-trans retinoic acid stealth liposomes prevent the relapse of breast cancer arising from the cancer stem cells. *J Control Release*. 2011;149:281–91.
 108. Ishida T, Iden DL, Allen TM. A combinatorial approach to producing sterically stabilized (stealth) immunoliposomal drugs. *FEBS Lett*. 1999;460:129–33.
 109. Singh SK, Bisen PS. Adjuvanticity of stealth liposomes on the immunogenicity of synthetic gp41 epitope of HIV-1. *Vaccine*. 2006;24:4161–6.
 110. Wang JC, Liu XY, Lu WL, Chang A, Zhang Q, Goh BC, Lee HS. Pharmacokinetics of intravenously administered stealth liposomal doxorubicin modulated with verapamil in rats. *Eur J Pharm Biopharm*. 2006;62:44–51.
 111. Amoozgar Z, Yeo Y. Recent advances in stealth coating of nanoparticles drug delivery systems. *Wiley Interdiscip Rev Nanomed Nanobiotechnol*. 2012;4:219–33.
 112. Dams ET, Laverman P, Oyen WJ, Storm G, Scherphof GL, Van Der Meir JW, Corstens FH, Boerman OC. Accelerated blood clearance and altered biodistribution of repeated injections of sterically stabilized liposomes. *J Pharmacol Exp Ther*. 2000;292(3):1071–9.
 113. Laverman P, Carstens MG, Boerman OC, Dams ET, Oyen WJ, Rooijen NV, Corstens FH, Storm G. Factors affecting the accelerated blood clearance of polyethylene glycol-liposomes upon repeated injection. *J Pharmacol Exp Ther*. 2001;298(2):607–12.
 114. Ishida T, Maeda R, Ichihara M, Irimura K, Kiwada H. Accelerated clearance of PEGylated liposomes in rats after repeated injections. *J Control Release*. 2003;88:35–42.
 115. Ishida T, Masuda K, Ichikawa T, Ichihara M, Irimura K, Kiwada H. Accelerated clearance of a second injection of PEGylated liposomes in mice. *Int J Pharm*. 2003;255(1-2):167–74.
 116. Ishida T, Ichikawa T, Ichihara M, Sadzuka Y, Kiwada H. Effect of physicochemical properties of initially injected liposomes on the clearance of subsequently injected PEGylated liposomes in mice. *J Control Release*. 2004;95(3):403–12.
 117. Ishida T, Harada M, Wang XY, Ichihara M, Irimura K, Kiwada H. Accelerated blood release of PEGylated li-

- posomes following preceding liposome injection: effects of lipid dose and PEG surface-density and chain length of first-dose liposomes. *J Control Release*. 2005;105(3):305–17.
118. Wang XY, Ishida T, Ichihara M, Kiwada H. Influence of the physicochemical properties of liposomes on the accelerated blood clearance phenomenon in rats. *J Control Release*. 2005;104(1):91–102.
 119. Ishida T, Ichihara M, Wang X, Yamamoto K, Kimura J, Majima E, Kiwada H. Injection of PEGylated liposomes in rat elicits PEG-specific IgM, which is responsible for rapid elimination of a second dose of PEGylated liposomes. *J Control Release*. 2006;112(1):15–25.
 120. Ishida T, Atoke K, Wang X, Kiwada H. Accelerated blood clearance of PEGylated liposomes upon repeated injections: effect of doxorubin-encapsulation and high dose first injection. *J Control Release*. 2006;155(3):251–8.
 121. Lavasanifar A, Samuel J, Kwon GS. Poly(ethylene oxide)-block-poly(L-amino acid) micelles for drug delivery. *Adv Drug Deliv Rev*. 2002;54:169–90.
 122. Batrakova EV, Kabanov AV. Pluronic Block Copolymers: Evolution of drug delivery concept from inert nanocarriers to biological response modifiers. *J Control Release*. 2008;130(2):98–106.
 123. Gaucher G, Dufresne MH, Sant VP, Kang N, Maysinger D, Leroux JC. Block copolymer micelles: preparation, characterization and application in drug delivery. *J Control Release*. 2005;109:169–88.
 124. Illum L, Davis SS. Effect of nonionic surfactant poloxamer 338 on the fate and deposition of polystyrene microspheres following intravenous administration. *J Pharm Sci*. 1983;72:1086–9.
 125. Illum L, Davis SS. The organ uptake of intravenously administered colloidal particles can be altered using a non-ionic surfactant (poloxamer 338). *FEBS Lett*. 1984;167:79–82.
 126. Illum L, Davis SS, Muller RH, Mak E, West P. The organ distribution and circulation time of intravenously injected colloidal carriers sterically stabilized with a block copolymer poloxamine 908. *Int J Pharm*. 1993;89:25–31.
 127. Rudt S, Muller RH. In vitro phagocytosis assay of nano and micro-particles by chemiluminescence III. Uptake of differently sized surface-modified particles and its correlation to particle properties and in vivo distribution. *Eur J Pharm Sci*. 1993;1:31–9.
 128. Moghimi S, Gray T. A single dose of intravenously injected poloxamine-coated long-circulating particles triggers macrophage clearance of subsequent dosage in rats. *Clin Sci (Lond)*. 1997;93(4):371–9.
 129. Moghimi SM, Pavey KD, Hunter AC. Real time evidence of surface modification of polystyrene lattices by poloxamine 908 in the presence of serum : in vivo conversion of macrophage prone nanoparticles to stealth entities by poloxamine 908. *FEBS Lett*. 2003;547:177–82.
 130. Dunn SE, Coombes AGA, Garnett MC, Davis SS, Illum L. In vitro cell interaction and in vivo distribution of poly(lactide-co-glycolide) nanosphere surface modified by poloxamer and poloxamine copolymers. *J Control Release*. 1997;44:65–76.
 131. Araujo L, Lobenberg R, Kreuter J. Influence of the surfactant concentration on the body distribution of nanoparticles. *J Drug Target*. 1999;6(5):373–85.
 132. Jain D, Athawale R, Bajaj A, Shrikhande S, Goel PN. Studies on stabilization mechanism and stealth effect of poloxamer 188 onto PLGA nanoparticles. *Colloids Surf B: Biointer*. 2013;109:59–67.
 133. Rapoport N. Physical stimuli-responsive polymeric micelles for anti-cancer drug delivery. *Prog Polym Sci*. 2007;32:962–90.
 134. He G, Ma LL, Pan J, Venkataraman S. ABA and BAB type tri-block copolymer of PEG and PLA: A comparative study of drug release properties and “stealth” particle characteristics. *Int J Pharm*. 2007;334:48–55.
 135. Moffatt S, Cristiano RJ. Uptake characteristics of NGR coupled stealth PEI/pDNA nanoparticles loaded with PLGA-PEG-PLGA tri-block copolymer for targeted delivery to human monocyte-derived dendritic cells. *Int J Pharm*. 2006;321:143–54.
 136. Zhiqing W, Wei L, Huibi X, Xiangliang Y. Preparation and in vitro studies of stealth PEGylated PLGA nanoparticles as carriers for Arsenic Trioxide. *Chin J Chem Eng*. 2007;15(6):795–801.
 137. Bazile D, Prud Homme C, Bassoullet M, Marlard M, Spenlehauer G, Veillard M. Stealth Me-PEG–PLA nanoparticles avoid uptake by the mononuclear phagocyte system. *J Pharm Sci*. 1995;84:493–8.
 138. Tobio M, Gref R, Sanchez A, Langer R, Alonso MT. Stealth PLA–PEG nanoparticles as protein carriers for nasal administration. *Pharm Res*. 1998;15:270–5.
 139. Govender T, Riley T, Stolnik S, Garnett MC, Illum L, Davis SS. PLA–PEG nanoparticles for site specific delivery: drug incorporation studies. *J Control Release*. 2000;64:269–347.
 140. Yarza TS, Formiga FR, Tamayo E, Pelacho B, Prosper F, Blanco-Prieto MJ. PEGylated-PLGA microparticles containing VEGF for long term drug delivery. *Int J Pharm*. 2013;440:13–18.
 141. Gref R, Miralles G, Dellacherie E. Polyoxyethylene coated nanospheres: effect of coating on zeta potential and phagocytosis. *Polymer Int*. 1999;48:251–6.
 142. Peracchia MT, Fattal E, Desmaele D, Bensard M, Noel JP, Gomis JM, Appel M, d’Angelo J, Couvreur P. Stealth PEGylated polycyanoacrylate nano-particles for intravenous administration and splenic targeting. *J Control Release*. 1999;60:121–8.
 143. Peracchia MT, Vauthier C, Puisieux F, Couvreur P. Development of sterically stabilized poly(isobutyl-2-cyanoacrylate) nanoparticles by chemical coupling of poly(ethylene glycol). *J Biomed Mater Res*. 1997;34:317–26.
 144. Peracchia MT, Vauthier C, Passirani C, Couvreur P, Labarre D. Complement consumption by poly(ethylene glycol)in different conformations chemically coupled topoly(isobutyl-2-cyanoacrylate) nanoparticles. *Life Sci*. 1997;61:741–61.
 145. Ahmed F, Discher DW. Self-porating polymersomes of PEG-PLA and PEG-PCL: hydrolysis-triggered controlled release vesicles. *J Control Release*. 2004;96:37–53.
 146. Jaeghere FD, Allemann E, Leroux JC, Stevels W, Feijen

- J, Doelker E, Gurny R. Formulation and lyoprotection of poly(lactic acid-co-ethylene oxide) nanoparticles: Influence on the physical stability and in vitro cell uptake. *Pharm Res.* 1999;16:859–66.
147. Vittaz M, Razile D, Spenlehauer G, Verrecchia T, Veillard M, Puisieux F, Labarre D. Effect of PEO surface density on long-circulating PLA–PEO nanoparticles which are very low complement activators. *Biomaterials.* 1996;17:1575–81.
148. Zambaux MF, Fiorina BF, Bonneaux F, Marchal S, Merlin JL, Dellacherie E, Labrude P, Vigneron C. Involvement of neutrophilic granulocytes in the uptake of biodegradable non-stealth and stealth nanoparticles in guinea pig. *Biomaterials.* 2000;21:975–80.
149. Butsele KV, Morille M, Passirani C, Legras P, Benoit JP, Varshney SK, Jerome R, Jerome C. Stealth properties of poly(ethylene oxide) based triblock copolymer micelles : A prerequisite for a pH-triggered targeting system. *Acta Biomaterialia.* 2011;7:3700–7.
150. Salmaso S, Caliceti P. Stealth properties to improve therapeutic efficacy of drug nanocarriers. *Drug Deliv.* 2013;2013:1–19.
151. Cabral H, Kataoka K. Progress of drug-loaded polymeric micelles into clinical studies, *J Control Rel.* 2014;190:465–76.
152. Muhlen A, Schwarz C, Mehnert W. Solid lipid nanoparticles (SLN) for controlled drug delivery: drug release and release mechanism. *Eur J Pharm Biopharm.* 1998;45(2):149–55.
153. Bocca C, Caputo D, Cavalli R, Gabriel L, Miglietta A, Gasco MR. Phagocytic uptake of fluorescent stealth and non-stealth solid lipid nanoparticles. *Int J Pharm.* 1998;175:185–93.
154. Madan J, Pandey RS, Jain V, Katore OP, Chandra R, Katyal A. Poly(ethylene)-glycol conjugated solid lipid nanoparticles improve biological half-life, brain delivery and efficacy in glioblastoma cells. *Nanomed. Nanotechnol.* 2013;9(4):492–503.
155. Tomalia DA, Baker H, Dewald J, Hall M, Kallos G, Martin S, Roeck J, Ryder J, Smith P. A new class of polymers: Starburst-dendritic macromolecules. *Polym J.* 1985;17:117–32.
156. Mignani S, Kazzouli SE, Bousmina M, Majoral JP. Expand classical drug administration ways by emerging routes using dendrimer drug delivery systems: A concise overview. *Adv Drug Deliv Rev.* 2013;65:1316–30.
157. Kojima C, Kono K, Maruyama K, Takagashi T. Synthesis of polyamidoamine dendrimers having poly(ethylene glycol) grafts and their ability to encapsulate anticancer drugs. *Bioconj Chem.* 2000;11:910–17.
158. Mallik N, Wiwattanapatapee R, Klopsch R, Lorenz K, Frey H, Weener JW, Meijer EW, Paulus W, Duncan R. Dendrimers: Relationship between structure and biocompatibility in vitro, and preliminary studies on the biodistribution of 125I-labelled polyamidoaminated dendrimers in vivo. *J Control Release.* 2000;65:133–48.
159. Chandrasekar D, Sistla R, Ahmad FJ, Khar RK, Diwan PV. The development of folate-PAMAM dendrimer conjugates for targeted delivery of anti-arthritis drugs and their pharmacokinetics and biodistribution in arthritic rats. *Biomaterials.* 2007;28:504–12.
160. Gajbhiye V, Palanirajan VK, Tekade RK, Jain NK. Dendrimers as therapeutic agents: a systematic review. *J Pharm Pharmacol.* 2009;61:989–1003.
161. Gong E, Matthews B, McCarthy T, Chu J, Holan G, Raff J, Sacks S. Evaluation of dendrimer SPL7013, a lead microbicide candidate against herpes simplex viruses. *Antiviral Res.* 2005;68:139–46.
162. Rupp R, Rosenthal SL, Stanberry LR. VivaGel™ (SPL7013 Gel): A candidate dendrimer – microbicide for the prevention of HIV and HSV infection. *Int J Nanomed.* 2007;2(4):561–6.
163. Liu Z, Davis C, Cai W, He L, Chen X, Dai H. Circulation and long-term fate of functionalized, biocompatible single-walled carbon nanotubes in mice probed by Raman spectroscopy. *Proc Natl Acad Sci. USA.* 2008;105(5):1410–15.
164. Prencipe G, Tabakman SM, Welsher K, Liu Z, Goodwin AP, Zhang L, Henry J, Dai H. PEG branched polymer for functionalization of nanomaterials with ultra-long blood circulation. *J Am Chem Soc.* 2009;131:4783–7.
165. Niidome T, M. Yamagata, Y. Okamoto, Y. Akiyama, H. Takahashi, T. Kawano, Y. Katayama, Y. Niidome. PEG modified gold nanorods with a stealth character for in vivo applications. *J Control Release.* 2006;114:343–7.
166. Akiyama Y, Mori T, Katayama Y, Niidome T. The effects of PEG grafting level and injection dose on gold nanorod biodistribution in tumor-bearing mice. *J Control Release.* 2009;139(1):81–4.
167. Zhou Z, Ma X, Jin E, Tang J, Sui M, Shen Y, Kirk EAV, Murdoch WJ, Radosz M. Linear-dendritic drug conjugates forming long-circulating nanorods for cancer drug delivery. *Biomaterials.* 2013;34(22):1–14.
168. Cho CS, Jeong YI, Ishihara T, Takei R, Park JU, Park KH, Maruyama A, Akaike T. Simple preparation of nanoparticles coated with carbohydrate carrying polymers. *Biomaterials.* 1997;18:323–6.
169. Maruyama A, Ishihara T, Kim SW, Akaike T. Nanoparticle DNA carrier with poly(L-lysine) grafted polysaccharide copolymer and poly(D,L-lactic acid). *Bioconj Chem.* 1997;8:735–42.
170. Fan C, Gao W, Chen Z, Fan H, Li M, Deng F, Chen Z. Tumor selectivity of stealth multi-functionalized superparamagnetic iron oxide nanoparticles. *Int J Pharm.* 2011;404:180–90.
171. Lee ES, Lim C, Song HT, Yun JM, Lee KS, Lee BJ, Youn YS, Oh YT, Oh KT. A nanosized delivery system of superparamagnetic iron oxide for tumor MR imaging. *Int J Pharm.* 2012;439:342–8.
172. Zhu L, Wang D, Wei X, Zhu X, Li J, Tu C, Su Y, Wu J, Zhu B, Yan D. Multifunctional pH-sensitive superparamagnetic iron-oxide nanocomposites for targeted drug delivery and MR imaging. *J Control Release.* 2013;169(3):228–38.
173. Kokuryo D, Anraku Y, Kishimura A, Tanaka S, Kano MR, Kershaw J, Nishiyama N, Saga T, Aoki I, Kataoka K. SPIO-PICosome : Development of a highly sensitive and stealth-capable MRI nano-agent for tumor detection

- using SPIO-loaded unilamellar polyion complex vesicles (PICsomes). *J Control Release*. 2013;169(3):220–7.
174. Hamidi M, Zarrin A, Forrozesh M, Mohammadi-Samani S. Application of carrier erythrocytes in delivery of biopharmaceuticals. *J Control Release*. 2007;118:145–60.
 175. Favretto ME, Cluitmans JCA, Bosman GJCGM, Brock R. Human erythrocytes as drug carriers: Loading efficiency and side effects of hypotonic dialysis, chlorpromazine treatment and fusion with liposomes. *J Control Release*. 2013;170:343–51.
 176. Holovati JL, Gyongyossy-Issa MIC, Acker JP. Effects of trehalose-loaded liposomes on red blood cell response to freezing and post-thaw membrane quality. *Cryobiol*. 2009;58(1):75–83.
 177. He H, Ye J, Wang Y, Liu Q, Chung HS, Kwon YM, Shin MC, Lee K, Yang VC. Cell-penetrating peptides mediated encapsulation of protein therapeutics into intact red blood cells and its application. *J Control Release*. 2014;176:123–32.
 178. Bae JS, Hwang MW, Kim IT, Lim CS, Ma KR, Kim YK, Lee KN, Kim DH, Byun SM. Chemical modifications of RBC surface antigen with methoxy polyethylene glycol. *Korean J Clin Pathol*. 1999;19:723–8.
 179. Scott MD, Murad K, Koumpouras F, Talbot M, Eaton JW. Chemical camouflage of antigenic determinants: Stealth erythrocytes. *Proc Natl Acad Sci USA*. 1997;94:7566–71.
 180. Murad KL, Mahany KL, Brugnara C, Kuypers FA, Eaton JW, Scott MD. Structural and functional consequences of antigenic modulation of red blood cells with methoxypoly(ethylene glycol). *Blood*. 1999;93:2121–7.
 181. Bradley AJ, Murad KL, Regan KL, Scott MD. Biophysical consequences of linker chemistry and polymer size on stealth erythrocytes: size does matter. *Biochim Biophys Acta*. 2002;1561:147–58.
 182. Bradley AJ, Scott MD. Immune complex binding by immune camouflaged poly(ethylene glycol)-grafted erythrocytes. *Am J Hematol*. 2007 Nov;82(11):970–5.
 183. Duncheng W, Kyliuk DL, Murad K, Toyofuku WM, Scott MD. Polymer-mediated immunocamouflage of RBC: Effects of polymer size on antigenic and immunogenic recognition of allogeneic donor blood cells. *Sci China Life Sci*. 2011;54:589–98.
 184. Wang D, Toyofuku WM, Scott MD. The potential utility of methoxypoly(ethylene glycol)-mediated prevention of rhesus blood group antigen RhD recognition in transfusion medicine. *Biomaterials*. 2012;33:3002–12.
 185. Chapanian R, Constantinescu I, Brooks DE, Scott MD, Kizhakkedathu JN. In vivo circulation, clearance and biodistribution of polyglycerol grafted red blood cells. *Biomaterials*. 2012;33:3047–57.
 186. Rossi NA, Constantinescu I, Kainthan RK, Brooks DE, Scott MD, Kizhakkedathu JN. Red blood cell membrane grafting of multi-functional hyperbranched polyglycerols. *Biomaterials*. 2010;31:4167–78.
 187. Scott MD, Chen AM. Beyond the red cell: PEGylation of other blood cells and tissues. *Transfusion Clinique et Biologique*. 2004;11:40–6.
 188. Bax BE, Bain MD, Talbot PJ, Parker-Williams EJ, Chalmers RA. Survival of human carrier erythrocytes in vivo. *Clin Sci*. 1999;96:171–8.
 189. Bax BE, Bain MD, Fairbanks LD, Webster ADB, Chalmers RA. In vitro and in vivo studies with human carrier erythrocytes loaded with polyethylene glycol-conjugated and native adenosine deaminase. *Brit J Haematol*. 2000;109:549–54.
 190. Chambers E, Mitragotri S. Prolonged circulation of large polymeric nanoparticles by non-covalent adsorption on erythrocytes. *J Control Release*. 2004;100:111–19.
 191. Rossi L, Castro M, D'Orio F, Damonte G, Serafini S, Bigi L, Panzani I, Novelli G, Dallapiccola B, Panunzi S, Di Carlo P, Bella S, Magnania M. Low doses of dexamethasone constantly delivered by autologous erythrocytes slow the progression of lung disease in cystic fibrosis patients. *Blood cells Mol. Dis*. 2004;33:57–63.
 192. Briones E, Colino CI, Millan CG, Lanao JM. Increasing the selectivity of amikacin in rat peritoneal macrophages using carrier erythrocytes. *Eur. J. Pharm. Sci*. 2009;38:320–4.
 193. Millan CG, Castaneda AZ, Lopez FG, Marinero MLS, Lanao JM. Pharmacokinetics and biodistribution of amikacin encapsulated in carrier erythrocytes. *J Antimicrob Chemoother* 2008;61:375–81.
 194. Yew NS, Dufour E, Przybylska M, Putelat J, Crawlet C, Foster M, Gentry S, Reczek D, Kloss A, Meyzaud A, Horand F, Cheng SH, Godfrin Y. Erythrocytes encapsulated with phenylalanine hydroxylase exhibit improved pharmacokinetics and lowered plasma phenylalanine levels in normal mice. *Mol Genet Metab*. 2013;109:339–44.
 195. Fan W, Yan W, Xu Z, Ni H. Erythrocytes load of low molecular weight chitosan nanoparticles as a potential vascular drug delivery system. *Colloids Surf. B*. 2012;95:258–65.
 196. Biagiotti S, Rossi L, Bianchi M, Giacomini E, Pierige F, Serafini G, Conaldi PG, Magnani M. Immunophilin-loaded erythrocytes as a new delivery strategy for immunosuppressive drugs. *J Control Release*. 2011;154:306–13.
 197. Harisa GI, Ibrahim MF, Alanazi F, Shazly GA. Engineering erythrocytes as a novel carrier for the targeted delivery of the anticancer drug paclitaxel. *Saudi Pharm J*. 2014;22:223–30.
 198. Hamidi M, Zarei N, Zarrin AH, Mohammadi-Samani S. Preparation and in vitro characterization of carrier erythrocytes for vaccine delivery. *Int J Pharm*. 2007;338:70–8.
 199. Madhavi BB, Bhavana M, Nath AR, Prasad M, Vennela KS. In vitro evaluation of piperine enclosed erythrocyte Carriers. *Drug Invention Today*. 2013;5(3):169–74.
 200. Hamidi M, Zarrin AH, Forrozesh M, Zarei N, Mohammadi-Samani S. Preparation and in vitro evaluation of carrier erythrocytes for RES-targeted delivery of interferon-alpha 2b. *Int J Pharm*. 2007;341:125–33.
 201. Ahn S, Jung SY, Seo E, Lee SJ. Gold nanoparticle-incorporated human red blood cells (RBCs) for X-ray dynamic imaging. *Biomaterials*. 2011;32:7191–9.
 202. Ma Y, Nolte RJM, Cornelissen JJLM. Virus-based nanocarriers for drug delivery. *Adv Drug Del Rev*. 2012;64:811–25.
 203. Cooper A, Shaul Y. Recombinant viral capsids as an ef-

- efficient vehicle of oligonucleotide delivery into cells. *Biochem Biophys Res Commun*. 2005;327(4):1094–9.
204. Broekman MLD, Comer LA, Hyman BT, Sena-Esteves M. Adeno-associated virus vectors serotypes with AAV8 capsid are more efficient than AAV-1 or -2 serotypes for widespread gene delivery to the neonatal mouse brain. *Neuroscience*. 2006;138:501–10.
 205. Wei F, McConnell KI, Yu T, Suh J. Cojugation of paclitaxel on adeno-associated virus (AAV) nanoparticles for co-delivery of genes and drugs. *Eur J Pharm Sci*. 2012;46:167–72.
 206. Selvam S, Thomas PB, Hamm-Alvarez SF, Schechter JE, Stevenson D, Mircheff AK, Trousdale MD. Current status of gene delivery and gene therapy in lacrimal gland using viral vectors. *Adv Drug Del Rev*. 2006;58:1243–57.
 207. Ren Y, Wong SM, Lim L. Folic acid-conjugated protein cages of a plant virus: A novel delivery platform for doxorubicin. *Bioconjug Chem*. 2007;18:836–43.
 208. Zeng Q, Wen H, Wen Q, Chen X, Wang Y, Xuan W, Liang J, Wan S. Cucumber mosaic virus as drug delivery vehicle for doxorubicin. *Biomaterials*. 2013;34:4632–42.
 209. Charoenphol P, Bermudez H. Design and application of multifunctional DNA nanocarriers for therapeutic delivery. *Acta Biomaterialia*. 2014;10:1683–91.
 210. Rothmund PWK. Folding DNA to create nanoscale shapes and patterns. *Nature*. 2006 Mar;440(16):297–302.
 211. Lo PK, Mettera KL, Sleiman HF. Self-assembly of three dimensional DNA nanostructures and potential biological applications. *Current opinion in chemical biology*. 2010;14:597–607.
 212. Ko SH, Liu H, Chen Y, Mao C. DNA nanotubes (DNA-NTs) as combinatorial vehicles for cellular delivery. *Biomacromolecules*. 2006;9(11):3039–43.
 213. Bhatia D, Mehtab S, Krishnan R, Indi SS, Basu A, Krishnan Y. Icosahedral DNA Nanocapsules by Modular Assembly. *Angew Chem Int Ed Engl*. 2009 May;48(23):413–7.
 214. Li J, Fan C, Pei H, Shi J, Huang Q. Smart drug delivery nanocarriers with self-assembled DNA nanostructures. *Adv Mater*. 2013;25:4386–96.
 215. Jiang Q, Song C, Nangreave J, Liu X, Lin L, Qiu D, Wang Z, Zou G, Liang X, Yan H, Ding B. DNA origami as a carrier for circumvention of drug resistance. *J Am Chem Soc*. 2012;134:13396–403.
 216. Kim K, Kim D, Lee T, Yhee JY, Kim B, Kwon IC, Ahn D. Drug delivery by self-assembled DNA tetrahedron for overcoming drug resistance in breast cancer cells. *Chem Commun*. 2013;49:2010–12.
 217. Chang M, Yang C, Huang D. Aptamer-conjugated DNA icosahedral nanoparticles as a carrier of doxorubicin for cancer therapy. *ACS nano*. 2011;5(8):6156–63.
 218. Choi K, Kwon IC, Ahn HJ. Self-assembled amphiphilic DNA-cholesterol/DNA-peptide hybrid duplexes with liposome-like structure for doxorubicin delivery. *Biomaterials*. 2013;34:4183–90.
 219. La TH, Nguyen TTT, Pham VP, Nguyen TMH, Le QH. Using DNA nanotechnology to produce a drug delivery system. *Adv Nat Sci: Nanosci Nanotechnol*. 2013;4:015002.
 220. Cheng X, Zhang F, Zhou G, Gao S, Dong L, Jiang W, Ding Z, Chen J, Zhang J. DNA/chitosan nanocomplex as a novel drug carrier for doxorubicin. *Drug Deliv*. 2009;16(3):135–44.
 221. Ouyang X, Li J, Liu H, Zhao B, Yan J, He D, Fan C, Chao J. Self-assembly of DNA-based drug delivery nanocarriers with rolling circle amplification. *Methods*. 2014;67:198–204.
 222. Nishikawa M, Mizuno Y, Mohri K, Matsuoka N, Rattanakit S, Takahashi Y, Funabashi H, Luo D, Takakura Y. Biodegradable CpG DNA hydrogels for sustained delivery of doxorubicin and immunostimulatory signals in tumor-bearing mice. *Biomaterials*. 2011;32:488–94.
 223. Andersen ES, Dong M, Nielsen MM, Jahn K, Subramani R, Mamdouh W, Golas MM, Sander B, Stark H, Oliveira CLP, Pedersen JS, Birkedal V, Besenbacher F, Gothelf KV, Kjems J. Self-assembly of a nanoscale DNA box with a controllable lid. *Nature Lett*. 2009;459:73–7.